K.F.N.

DEFENCE RESEARCH
TELECOMMUNICATIONS
ESTABLISHMENT

NOISE AND INTERMODULATION IN THE IONOSPHERIC SOUNDER RECEIVER FOR THE ALOUETTE AND ISIS SATELLITES (U)

by

Trond Endresen

DRTE TECHNICAL NOTE NO. 607

DEFENCE RESEARCH BOARD
DEPARTMENT OF NATIONAL DEFENCE
CANADA

DRTE TN NO. 607

OTTAWA

FEBRUARY 1969

02 DRTE, EL
02a 106975
02b TN 607

41 M

105-03842/

DEFENCE RESEARCH BOARD

DEPARTMENT OF NATIONAL DEFENCE
CANADA

02c DEFENCE RESEARCH TELECOMMUNICATIONS ESTABLISHMENT (Can)
02d (ELECTRONICS LABORATORY)
02e Ottawa Ont

09 57
09a 24

04/ NOISE AND INTERMODULATION IN THE IONOSPHERIC SOUNDER RECEIVER FOR THE ALOUETTE AND ISIS SATELLITES (U),

by

TROND ENDRESEN 11
Norwegian Defence Research Establishment, Oslo
(Summary of work as an NDRE Engineer seconded to DRTE 1966-67)

35 (D)-02-04-02

DRTE TECHNICAL NOTE NO 607

46 Feb 69

PROGO No. D02-04-02

Published February 1969
OTTAWA

CAUTION
"This information is furnished with the express understanding that:
(a) Proprietary and patent rights will be protected.
(b) It will not be released to another nation without specific approval of the Canadian Department of National Defence."

TABLE OF CONTENTS

	Page
ABSTRACT	1
1. Introduction	1
2. Definitions of Intermodulation	4
2.1 Intermodulation	4
2.2 Image Frequencies	5
2.3 Subharmonically Related Frequencies	6
3. Measuring Procedure for Intermodulation and Noise	8
3.1 Intermodulation	8
3.2 Noise	9
4. Intermodulation in Transistor Amplifiers	10
5. Mixers	13
6. Parametric Up-Converters	16
6.1 Introduction	16
6.2 General Theory	17
6.3 Noise	21
6.4 Bandwidth	24
6.5 Experimental Results	25
7. General System Considerations	27
8. References	29
9. Acknowledgements	30
APPENDIX A	31
APPENDIX B	34

LIST OF FIGURES AND TABLES

		Page
Figure 1	Antenna Impedance Versus Frequency.	36
Figure 2	Signal Strength at Receiver Terminals for Various Ground Transmitter Powers	
Figure 3	Setup for Intermodulation Checks	37
Figure 4	Typical Input-Output Characteristics	
Figure 5	Noise Figure Versus Source Impedance for Common Base Amplifier	38
Figure 6	Single Ended Common Base Amplifier	
Figure 7	Single Ended Common Base Amplifier with Diode Compensation	39
Figure 8	Push Pull Common Base Amplifier	
Figure 9	Push Pull Common Base Amplifier with Diode Compensation	40
Figure 10	Current Gain for 2N2501 (Normalized)	
Figure 11	Differential Amplifier	41
Figure 12	Balanced Wideband Mixer	
Figure 13	Mixer Assembly	42
Figure 14	Output Buffer Noise Figure Versus Source Impedance	43
Figure 15	Ring Mixer and Buffer	
Figure 16	Field Effect Transistor Mixer	44
Figure 17	Local Oscillator Square Wave Driver	
Figure 18	General Equivalent for a Reverse Biased Varactor Diode	45
Figure 19	Low Frequency Equivalent for a Reverse Biased Varactor Diode	
Figure 20	Equivalent Circuit for Parametric Up-Converter	46
Figure 21	Equivalent for Noise Calculations	
Figure 22	Equivalent for Noise Calculation	
Figure 23	Third Order Intermodulation in a Parametric Up-Converter Using Abrupt Junction Diodes	47
Figure 24	Typical Pumping Schemes for Parametric Up-Converter	48
Figure 25	Parametric Up-Converter	
Figure 26	Conversion of Parametric Up-Converter Shown in Figure 25	49

		Page
Figure 27	Minimum Detectable Sky Temperature for 240 Foot Dipole	50
Figure 28	Brightness Temperature from Cosmic Noise Versus Frequency (From Reference 23)	51
Figure 29	Antenna Equivalent	
Table 1	Intermodulation of Common Base Amplifiers	52
Table 2	Intermodulation of Differential Amplifier	
Table 3	Second Order Intermodulation Comparison of Switching Elements	
Table 4	Second Order Intermodulation Comparison of Series Resistance	53
Table 5	Second Order Intermodulation Versus Drive Level	54
Table 6	Additional Second Order Intermodulation Measurements	
Table 7	Noise Figure of Mixer Assembly	55
Table 8	Second Order Intermodulation for Different Local Oscillator Impedances	56
Table 9	Second Order Intermodulation in Field Effect Transistor Mixers	57
Table 10	Intermodulation in Parametric Up-Converter	

NOISE AND INTERMODULATION IN THE IONOSPHERIC SOUNDER RECEIVER FOR THE ALOUETTE AND ISIS SATELLITES

A B S T R A C T

The problems associated with sounding the topside of the ionosphere over a wide frequency range with limited transmitter power and a long extendible electric dipole antenna system are described.

Estimated interference levels from ground based HF transmitters are given, and the effects of such interference on the sounder receiver are described.

Noise figures for various receiver front-ends are given when driven by an electrically short antenna having a source impedance which is large and essentially capacitive.

Intermodulation and noise characteristics for different transistor amplifiers, resistive mixers and parametric up-converters are also given.

1. INTRODUCTION

The main experiment in the Canadian Alouette and ISIS satellites is a swept frequency ionospheric topside sounder. The sounding principle used in these satellites is as follows: a pulsed RF signal of frequency f_o is transmitted vertically down into the ionosphere. When it reaches a region of electron density given by the expression(3)

$$N_e = \frac{f_o^2}{80.5}$$

where N_e = electrons/cm^3

and f_o = frequency in kHz,

and if we neglect the effect of the earth's magnetic field, the signal will be totally reflected and the time spent for the signal to travel down and up again is measured. If the frequency f_o is swept, one can generate a display or ionogram in the form of plasma frequency (and therefore electron density) vs distance of reflection level from the satellite. Simultaneously a plot of the cosmic noise level is obtained from the AGC output of the receiver.

The frequency range required for sounding is from approximately 20 MHz to as far below 1 MHz as possible. In Alouette II the sounding receiver frequency range was from 0.13 MHz to approximately 14.5 MHz. The antenna system used for this bandwidth consists of two crossed Hertzian dipoles measuring 75 ft. and 240 ft. tip-to-tip respectively. These antennas are connected to the transmitter and to the receiver via a T/R switch and a cross-over network. For ISIS-C - a magnetospheric satellite to be launched in 1972-73, the intention is to sound from 10 kHz-20 MHz. In addition, the satellite will be put into an elliptical orbit with a perigee similar to that of Alouette II (i.e. 500 km) and an apogee of the order of 15-20 earth radii. Extending the sounding frequency range down to 10 kHz will necessarily put severe limitations on system performance at the low end of the band. The use of a single receiving system for both ionospheric sounding and cosmic noise measurements compromises and complicates the receiver design and it would be much easier to perform the cosmic noise and sounder measurements using separate receivers.

In the sounding system we have two major problems, firstly, the "echo" signal from the ionosphere has to overcome the cosmic noise level appearing on the antenna terminals. Secondly the system noise temperature at the receiver preamplifier input terminals must not be set by the effective receiver noise temperature. With the receiving system used in Alouette II the lowest frequency at which cosmic noise measurements can be made is around 600 kHz. Below this frequency the effect of increasing antenna mismatch loss and relatively high sounder receiver noise figure results in the cosmic noise being masked by receiver noise. In addition, a beat-frequency between the two VHF telemetry transmitters gives a serious interference signal centred at 510 kHz. At first it seemed likely that much of this telemetry interference could have been eliminated by the addition of VHF traps at the input terminals of the Alouette II receiver. It now seems however, that the non-linearity of the plasma will ensure generation of this beat frequency signal.

There are three obvious solutions to the signal-noise problem at low frequencies. The first is to raise the peak power of the transmitter pulse, the second is to reduce the antenna mismatch loss by making the antenna dipoles longer, and the third is to make the transmitter pulse longer and the receiver IF and post-detection bandwidths narrower. The first and third suggestions both involve higher average transmitter powers while the first suggestion of course has the added complication of higher peak power. Increasing the transmitted power also raises power supply problems since a doubling of the average transmitter power, for example, will only raise the signal/noise ratio 3 db while doubling the power drawn from the spacecraft batteries. A major improvement in signal/noise ratio could be obtained by the second approach, i.e. making the antennas longer. But here again one will come up against serious practical problems in the form of mechanical constraints, and experience in Canada and the U.S. suggests that a practical upper limit at the present time is about 2000 ft. tip-to-tip for a sounder dipole.* As an

* The U.S. Radio Astronomy Explorer satellite to be launched in 1968 will have two extendible tubular V antennas, the largest V having a pole length of 750 feet.

example of the antenna impedance problems at low frequencies, a plot of the resistive and the reactive part of the impedance vs frequency (from 10 kHz - 1 MHz) for the 240 ft. dipole in Alouette II is shown in Figure 1. It should be mentioned that these are computed results and assume free space conditions. When the antennas are embedded in a plasma, at frequencies near and below the plasma frequency, the impedance can be quite different from the free space values. These working conditions frequently occur for Alouette I and II and the effect on antenna impedance is at present largely unknown. In addition to noise and mismatch problems the sounder system can, at times, experience severe interference from ground based HF transmitters. One finds that when the satellites pass regions with high broadcasting activity that the ionograms and the AGC records can be badly degraded by this type of interference. T.R. Hartz[1] has made a systematic analysis of the AGC records from Alouette I and has shown good evidence of high correlation between ionogram interference and transmissions from HF transmitters on the ground. He found that night time interference was much higher than that appearing in the daytime, and concludes from his study that interfering frequencies must be in the frequency range above the F layer penetration frequency (f_oF_2), Very good correlation appeared between these interference phenomena and f_oF_2. On the basis of some obviously uncorrelated frames it was concluded that D layer absorption was probably unimportant. From an experiment made it was also found that it was unlikely that there would be significant interference due to signals propagating through the ionosphere by the whistler mode.

Data from the Alouette II satellite supports this analysis. The important difference between Alouette I and II with respect to interference is the insertion of three bandpass filters in the preamplifier in Alouette II to provide better interference protection. The filters cover the frequency ranges 0.1 - 2.0 MHz, 2.0 - 7.0 MHz and 7.0 - 15 MHz respectively.

An investigation by H. Kowalik[2] shows that interference from ground-based transmitters is to be expected. For example, in the frequency band 9.50 - 9.73 MHz (i.e. half of 19 MHz, the frequency of the first IF in Alouette I and II) there are more than 350 transmitters with transmitted powers greater than 1 kw distributed around the world, and there are 54 channels in this band separated by 5 kHz. 50% of them have more than 50 kW output power and some more than 150 kW. Typical antenna gains are about 22 db, fan beamwidths 35° (3 db points) and elevation angles are typically between 7° and 20° depending on frequency. Kowalik[2] made calculations for the Alouette I antenna system to get an approximate figure for interference levels and made the following assumptions

(1) elevation angle to the satellite = 15°

(2) distance to the satellite = 1450 statute miles

(3) transmitter antenna gain = 20 db

(4) satellite antenna gain an average of 2 db

(5) polarization loss = 3 db

(6) losses in the spacecraft antenna matching network = 10 db

(7) input impedance of the sounder receiver = 400 ohms from 1 - 10 MHz.

The results are shown in Figure 2. Although the transmitter antenna gain of 20 db for the lower part of the frequency range is quite unrealistic, the calculations should in practice provide a good basis for assessing interference probabilities in the sounder system since low frequencies will not normally penetrate the ionosphere. We will come back to Figure 2 later. For the present we will only state that for a 1 MW transmitter located on the ground, interference levels across 400 ohms receiver input terminals can be as high as 50 - 60 mV in Alouette I, and 160 - 200 mV in Alouette II. The increased level in Alouette II is due to the fact that the received voltage is proportional to the length of the antenna as long as the antenna is matched. The gain for matched conditions only changes slightly with frequency: for an infinitesimal dipole the gain is equal to 1.5, for a half-wavelength dipole it is 1.64. In addition, Alouette II's 500 km perigee is half that for Alouette I (1000 km) (see also Appendix B in this report).

2. DEFINITIONS OF INTERMODULATION

There are several types of distortion phenomena in a receiver system. For the present application we have mainly three general types of interference which can give us unwanted distortion, namely;

(1) intermodulation

(2) image frequencies

(3) frequencies at or subharmonically related to the IF of the receiver.

Effects of cross modulation on the performance of a receiver have never been observed in practice and can probably be neglected. This is essentially due to post detection filtering of the desired short pulse signals.

2.1 INTERMODULATION

In the stages ahead of the first mixer the most serious intermodulation occurs when two or more high level unwanted signals are present on the antenna terminals simultaneously and have frequencies such that their fundamentals or harmonics can be combined to give the frequency the receiver is tuned to, its image frequency, or a frequency within the pass-band of the first IF crystal filter.

In the mixer the problem will be slightly different: If two or more unwanted signals are present and their fundamental frequencies or harmonics combine with the LO frequency or harmonics of it to give a mixing product

inside the IF crystal filter bandwidth, we can get serious interference. Even worse is the case when the mixing product is equal to the IF frequency without the LO taking part. According to Hartz's report[1] this may be the main interference mechanism in the Alouette I satellite. Typical combinations in the pre-mixer stages are then:

$$f_1 \pm f_2 \approx f_o, \quad \text{second order IM}$$

$$2f_1 \pm f_2 \approx f_o, \quad \text{third order IM}$$

$$Mf_1 \pm Nf_2 \approx f_o, \quad M + N \text{ order IM}$$

In the mixer,

$$f_{LO} - (f_1 \pm f_2) \approx f_{LO} - f_o = f_{IF}, \quad \text{second order IM}$$

$$f_{LO} - (2f_1 \pm f_2) \approx f_{LO} - f_o = f_{IF} \quad \text{third order IM}$$

$$f_{LO} - (Mf_1 \pm Nf_2) \approx f_{LO} - f_o = f_{IF}, \quad M + N \text{ order IM}$$

$$L\, f_{LO} - (Mf_1 \pm Nf_2) \approx f_{LO} - f_o = f_{IF}$$

where L, M and N are integers.

In addition, in the mixer we can have

$$Mf_1 \pm Nf_2 \approx f_{IF}$$

f_1, f_2 = interfering frequencies

f_o = the frequency the receiver is tuned to

f_{IF} = the IF

f_{LO} = local oscillator frequency

In these examples we have assumed a lower sideband up-converter

where $f_{IF} = f_{LO} - f_{sig}$

and $f_{LO} > f_{IF} > f_{sig}$.

2.2 IMAGE FREQUENCIES

In a double conversion receiver both first and second IF image responses are possible. If the front end has an inadequate low pass filter then signals at $f_{LO_1} + f_{IF_1}$ will be frequency translated in the first mixer to f_{IF_1}. The wanted signals are of course at $f_{LO_1} - f_{IF_1}$ and we call $f_{LO_1} + f_{IF_1}$ its image

in the first IF. In the ISIS-A satellite the local oscillator sweeps to within 100 kHz of f_{IF} hence the minimum image frequency is $\simeq 2\ f_{IF_1}$. The front end of the receiver should therefore have a low-pass filter with an f_{co} just beyond the upper end of the sounding frequency range and having the highest possible attenuation at frequencies $\geq 2\ f_{IF_1}$. The antenna system will be quite sensitive to such out of band signals and will become increasingly directional as the frequency increases i.e. as the antenna becomes many wavelengths long. No data is presently available on antenna losses at VHF and UHF.

If the first IF has inadequate bandpass filtering, signals at $f_{LO_1} - f_{IF_1} + 2\ f_{IF_2}$ will be amplified in the first IF and frequency translated to f_{IF_2}. For example, suppose the wanted signal

$$f_s = 1.5 \text{ MHz}$$

and let

$$f_{IF_1} = 19 \text{ MHz}$$

$$f_{IF_2} = 0.5 \text{ MHz}$$

Then

$$f_{LO_1} = 20.5 \text{ MHz} = \text{first local oscillator}$$

$$f_{LO_2} = 18.5 \text{ MHz} = \text{second local oscillator}$$

When $f_I = 2.5$ MHz

then $f_{LO_1} - f_I = 18.0$ MHz

and $f_{LO_2} - 18.0 = 0.5 \text{ MHz} = f_{IF_2}$

f_I is therefore called the image of f_s in the second IF.

Second IF image attenuation for Alouette II was 65 db and was achieved using a single xtal filter immediately following the first local oscillator. First IF image attenuation in Alouette II was set by bandpass filters in a preamplifier and was $\geq$ 50 db to about 50 MHz with no measurements taken beyond this frequency.

2.3 SUBHARMONICALLY RELATED FREQUENCIES

Frequencies of the following type can also give interference;

$$n \cdot f_1 \approx f_o \text{ or } f_{IF}$$

Generally most of the interference distortion is expected to come from second and third order intermodulation. Second order terms can, to a certain extent, be suppressed by octave band switched filters in front of the pre-amplifier. There are however three general limitations to such a filtering scheme. Firstly, one does not know precisely the impedance of an antenna imbedded in a plasma, and it will also change throughout the orbit because of changing electron density. This will put a limit on the effective skirt selectivity achievable with a given number of elements. This situation becomes particularly serious at and below plasma frequencies. In addition, one requires less than octave-band filtering because of finite skirt selectivity Secondly, filters have a finite insertion loss and can give a significant noise contribution when put in front of the first preamplifying stage.

The third problem is the T/R switch. Because of the high RF output voltage of the transmitter it is highly desirable to put this circuit in front of the filter to avoid breakdown problems in filter components. Therefore the requirement for the T/R switch must be that it can stand the full interference level without introducing significant harmonic and intermodulation distortion.

In addition to the problems mentioned here there are others in connection with particular preamplifier configurations, and these will be mentioned later.

Third order IM can never be eliminated by octave filtering because the interfering signals can lie arbitrarily close to the wanted signal. To reduce the probability of third order IM one must use narrower front end filters. Let us consider a simple calculation showing the dependence of third order IM on filter bandwidth.

We assume the interference signal distribution to be constant over the whole band and to have a probability density equal to d per unit bandwidth. The probability of finding a signal inside the filter pass band is then:

$$p_1 \propto \Delta f \cdot d$$

The equation giving the interference of third order is:

$$f_o - \frac{\Delta f}{2} \leq 2f_1 - f_2 \leq f_o + \frac{\Delta f}{2}$$

or

$$f_o + \frac{\Delta f}{2} + 2f_1 \geq f_2 \geq f_o - \frac{\Delta f}{2} + 2f_1$$

f_o is a frequency in the filter bandwidth Δf, and is here arbitrarily chosen to be the center frequency. f_1 and f_2 are interfering signals.

The probability of having a frequency f_2 between these limits is then

$$p_2 \propto \Delta f \cdot d$$

and the probability for interference by

$$f_{out} = 2f_1 - f_2$$

is then (because of mutual independence)

$$p_o \propto (\Delta f \cdot d)^2 \propto \Delta f^2$$

Generally one can say that after the unwanted signals have passed the pre-filtering stages, the only way to reduce distortion is to increase the dynamic range and reduce the nonlinearities.

It should be mentioned that in addition to these different phenomena due to external signals, we can have internally generated spurious responses, for example due to a frequency synthesizer or from other experiments and equipment (e.g. telemetry transmitters) in the satellite. These problems will not be taken into consideration here.

3. MEASURING PROCEDURE FOR INTERMODULATION AND NOISE

3.1 INTERMODULATION

A good indication of the linearity of the sounder-system can be obtained by measuring its second and third order intermodulation products. The technique used to measure these intermodulation products will be described shortly, see Figure 3.

Two HP 606A generators were terminated using two fixed 10 db pads and two 1 db-step attenuators connected together via a three-port 50 ohm coupling unit, i.e. when two ports are terminated with 50 ohms, the third port has an input impedance of 50 ohms. The third port was connected to a low-pass filter. This filter was again terminated in a suitable matching network to keep the 50 ohm cable properly terminated and to get the proper source impedance for the circuit under test. The voltage at the output of this matching unit is then the reference level. The connection between the matching network and the circuit under test must be kept short. The frequencies were always measured with a counter.

With the precautions mentioned here this system can measure IM figures up to 105 db above a reference level of 1μV into 50 ohms.

The measuring procedure is as follows:

The output voltage is set to zero on one of the generators. The other one is set to the wanted frequency and reference level. If the circuit under test is a mixer, the LO frequency is set to maximum output IF reading on a selective μV-meter. The output level is noted.

Then both generators are tuned to frequencies separated by the frequency the system is tuned to (in case of second order intermodulation). The levels are then increased simultaneously to an output equal to the reference level of one generator on the wanted frequency. The level of each generator above the input reference level is then the intermodulation rejection of the system. The same procedure is used for third order terms e.g. $2f_1 \pm f_2$.

The reference level must always be known when a certain intermodulation figure is given. When measuring parts of a cascaded system, one has to adjust the reference level on the different test points according to the voltage levels in the complete system. The right source impedance must also be used otherwise very misleading results can be obtained, for example, parts of a system can show poorer intermodulation than the complete system. Usually in the literature the tangential sensitivity level is defined as the reference level. But as long as the sensitivity is dependent on the bandwidth, the absolute value of the reference level must be given to obtain any definite information about the interference level the system can stand. In the measurements presented in this report, a reference level of 2 μV in series with an antenna resistance of 400 ohms has been used for preamplifier tests. This allows comparison with measurements done earlier in this laboratory, which used 1 μV reference at the input terminals of preamplifiers with a 400 ohm input resistance. The antenna resistance was also 400 ohms. This level has then been adjusted for different test points in the mixer and buffer amplifiers assuming reasonable power gain or loss. Using a reference voltage level in series with a certain resistance will be the most meaningful reference for comparing systems. Using the power into the device will be meaningless for a high input impedance circuit such as a field-effect transistor amplifier.

Because of the high level of the interfering signals and the high LO drive used, extreme precautions must be taken in layout, shielding, and proper grounding techniques. If this is not done the true limitations of the system will not show up and repeatable results will not be obtained.

3.2 NOISE

Tangential sensitivity is in this report defined as the additional voltage, V_1, on the input terminals of the circuit under test necessary to raise the output power level 3 db above the noise-level. From this value the noise figure can be obtained in the following way if the input is matched:

$$NF = \frac{\frac{V_1^2}{R_s}}{kTB}$$

V_1 = tangential sensitivity

R_s = source impedance (matched)

k = Bolzmann's constant

T = temperature of the source resistance

B = bandwidth

If the input is not matched one has to take the Thevenin equivalent of the signal circuit when the output is increased 3 db, let us say we then have a voltage V(rms) in series with a resistance R_s. The noise figure will then be (5):

$$NF = \frac{\frac{V^2}{4R_s}}{kTB}$$

In most cases in the present work a noise generator has been used and this is calibrated to give noise figure levels directly in db. In Appendix B the definitions for brightness temperature, antenna temperature, effective temperature, and system temperature will be found.

4. INTERMODULATION IN TRANSISTOR AMPLIFIERS

There are two general causes of intermodulation, namely saturation effects and nonlinearities, and it is often difficult to separate these two phenomena. The concept of dynamic range is illustrated in Figure 4. The distortion caused by saturation will be directly related to the dynamic upper limit for the system.

Let us take an amplifying device for example. When the signal levels approach the level for saturation, the input/output characteristics can be represented by a power series of the following form:

$$V_{out} = k_1 \cdot V_{in} + k_2 \cdot V_{in}^2 + k_3 V_{in}^3 + \ldots + k_n \cdot V_{in}^n$$

The coefficients can be a function of the bias for example in a transistor amplifier. We express V_{in} in the following form to be able to easily pick out the frequencies in the output:

$$\left[V_{in} = \frac{1}{2} \quad V_1 \cdot e^{j\omega_1 t} + V_1 \cdot e^{-j\omega_1 t} + V_2 \cdot e^{j\omega_2 t} + V_2 \quad e^{-j\omega_2 t}\right]$$

One second order term will then be:

$$\left|V_{out}\right| \propto k_2 \quad \left|V_1\right| \cdot \left|V_2\right|$$

Similar contributions will come from all the even order terms in the power series. The third order contribution will typically be of the following form:

$$\left|V_{out}\right| \propto k_3 \quad \left|V_1\right|^2 \cdot \left|V_2\right|$$

Similar contributions will come from all the odd order terms in the power series. If we assume that the series can be terminated after the third term, the intermodulation from this type of distortion source will have the following characteristics (assuming $\left|V_1\right| = \left|V_2\right|$):

Second order IM is proportional to the signal squared, and third order is proportional to the signal cubed.

The same dependence on signal level will be observed for all non-linearities of this type. For example, in a field-effect transistor the transfer characteristics is approximately of this form:

$$i_D = k_1 \cdot e_{in} + k_2 \cdot e_{in}^2 + k_3 \cdot e_{in}^3$$

where $k_3 \not< k_2$

This characteristic will always give distortion no matter how great the dynamic range is.

There are generally at least four nonlinear effects in bipolar transistors that can give distortion, namely:

(1) emitter resistance dependent on emitter current

(2) current gain dependent on emitter current

(3) current gain dependent on collector-base voltage

(4) nonlinear collector-base capacity

An extensive study and analytical treatment of these effects using an accurate large-signal model for the transistor has, to the author's knowledge, not yet been published. This is not surprising because of the complexity of the problem and the mathematical difficulties involved. Even assuming you have a high speed computer available, you are still left with a difficult modelling problem, and your results are of course completely dependent on the accuracy of your model.

The present opinion in this laboratory is that using a CDC 3200 computer with one of the big network analysis programs, such as SCEPTRE, will probably be of some value in comparing different circuit configurations and pinpointing weak design areas. It is likely that SCEPTRE will eventually be available to the DRTE Computing Centre, and an effort will be made to use it for intermodulation calculations.

The approach, so far, to the investigation of the different circuits has therefore been mostly of an experimental nature based on a good physical understanding of the basic mechanisms involved. In dealing with these distortion problems, it is worth noting that an improvement in the intermodulation characteristics is usually accompanied by an increase in noise figure. Hence, low noise and wide dynamic range tend to be conflicting requirements. The first thing to take into account when designing a transistor stage with low intermodulation distortion is the dc biasing. The emitter current bias must be high enough to avoid saturation effects but not so high as to produce an excessive increase in noise figure. The next thing to consider is the variation of current gain, h_{fe}, versus emitter current, and to pick a transistor, and an operating region, where the h_{fe} vs emitter current is reasonably flat.

The nonlinearity in C_{ob} with voltage did not seem to be a dominant factor for distortion in the circuits described in this report. In the cases where very good intermodulation figures showed up, the collector voltages were varied. No difference in intermodulation appeared. This nonlinear effect must therefore be "swamped out" by other distortion mechanisms. If the load impedance is high the C_{ob} nonlinearity will probably show up. The types of preamplifier configurations using bipolar transistors that have been taken into consideration for the sounder receiver are mainly:

(1) common-base single ended

(2) common-base push-pull

(3) differential amplifier

(4) feedback configurations

The push-pull circuit has an advantage over the single ended version in that it gives some cancellation of second order intermodulation terms in the output transformer. This transformer must therefore by very well balanced for the whole frequency band. Theoretically, some advantage should be gained by driving these types of circuits from a current source to counteract the nonlinear emitter-base characteristic. But the source impedance cannot be raised too much without significantly degrading the noise figure. A curve showing typical variation of noise figure versus source impedance for a push-pull common base amplifier is shown in Figure 5.

Measurements were taken to compare the common base single ended configuration with the push-pull common base amplifier (both with and without compensating diodes). 2N2501 transistors were used and the relevant circuits are shown in figures 6, 7, 8 and 9. The resistance in series with the emitters and the load were kept constant. The two push-pull amplifiers used the same transformers. In this way the figures obtained for intermodulation rejection should be directly comparable. In the measurement, 3 μV was used as the reference level in order to keep the output well above the μV meter noise level.

Low-pass filters (f_{co} = 1.5 MHz and 4.5 MHz) were inserted in front of the μV meter (Rohde and Schwarz) to avoid intermodulation in the meter (interfering signals have to be below 1 mV). In assuming a nonlinearity of the following form has caused the intermodulation

$$V_{out} = k_1 V_{in} + k_2 \cdot V_{in}^2 + k_3 \cdot V_{in}^3$$

the intermodulation can be referred to 1μV at the input. The results are shown in Table 1.

Figure 10 shows measured values of β_{DC} (h_{FE}) and β (h_{fe}) at 20 MHz versus emitter current for a 2N2501 transistor. The reason for choosing this particular transistor is that β is relatively flat around a reasonably high emitter current. When these transistors were used in pairs they were selected, i.e. matched, for similar characteristics.

From Table 1 it is quite obvious that the third order IM is relatively independent of compensating diodes and a push-pull configuration and is what we should expect. For the second order IM terms the compensating diode gives between 12 and 18 db improvement, and the push-pull arrangement gives even more improvement, between 15 and 18 db over the single ended configuration. The measurements show also that using compensating diodes in a push-pull configuration will give little or no advantage if both the emitter currents and the rf voltages on the two sides are adjusted for good balance. A differential amplifier, Figure 11, was measured at different frequencies for various values of emitter-resistances R_1 and R_2. This circuit was easy to balance and it showed good broadband characteristics. IM results are shown

in Table 2. An increase in the load from 200 to 800 ohms changed the performance only slightly.

Feedback amplifiers of different kinds are presently under investigation in the laboratory.

5. MIXERS

The weakest point in the receiver front end seems to be the mixer. Measurements done in this laboratory and other establishments indicate wideband transistor amplifiers are easier to design for low intermodulation distortion than wideband mixers. Generally one has to trade off between noise and intermodulation. The constraints put on the mixer were mainly:

(1) noise figure as low as possible,

(2) very high dynamic range for good intermodulation rejection,

(3) biasing should not be more critical than for the rest of the system,

and (4) double balancing needed, i.e. both for signal and local oscillator.

A switched diode ring mixer (ref. 6 to 13) was found to be a promising solution, and such a circuit was used in both Alouette I and II. (See Figure 12 for the Alouette II mixer.)

Ideally if we assume the diodes switching between zero and infinite resistance and solely controlled by the LO current (diode switching not affected by signal currents), we should have no intermodulation at all. The best approximation to these conditions is to drive the diodes with a large amplitude LO current source, to use very fast diodes with low charge storage and to have a high source impedance in the signal line to the diodes.

The reason for using a signal current source is to avoid any influence on the current waveform from changing diode resistance (12). The main contribution to intermodulation should then be due to finite signal currents perturbing the LO switching of the diodes.

Other contributions to intermodulation can be charge storage effects, finite voltages across output load resistance of the mixer tending to unbalance the diodes, non-ideal current sources due to shunt losses in transformers, etc.

The mixer circuits should also display good balance over a wide band and this is achieved by matching diodes and taking exceptional care in balancing transformer windings. Balancing of the signal line provides useful attenuation of harmonic and intermodulation products at the IF frequency generated in the premixer stages.

The mixer assembly in Figure 12 was measured with a 50 ohm source impedance and showed a typical value of approximately 70 db for second order intermodulation. This figure can be improved for the whole band, .1 - 18 MHz, by using resistors in series with the diodes. Narrowband improvement can be obtained if one carefully balances the ring with small capacitors to ground from different points in the ring, by selecting an optimum LO drive level (not necessarily as high as possible) and by putting small dc voltage biases on the diodes. The intermodulation figure is also of course dependent on the type of diodes used. The results of the measurements on this circuit will be mentioned later in the general discussion.

We will now look more thoroughly into a slightly different switched diode mixer, see Figure 13. This circuit was used for the set of measurements shown in Tables 3-8.

The following are some comments on these measurements:

(1) The emitter resistances in the input buffer were adjusted to give an intermodulation rejection better than for the mixer itself. The IM figure for the buffer was then better than 85 db for all frequency combinations measured. The intermodulation test was done with full LO drive through the diodes, 42 mA through each diode (0-peak current).

(2) The output buffer had an IM figure better than 76 db for all frequency combinations measured. To be sure a possible LO leak should not destroy this figure or that this figure of 76 db was not limiting the overall performance, an attenuation network of 20 times was put in the output buffer keeping the input impedance constant. Repetition of some IM figure measurements for the whole mixer assembly showed no change.

(3) Leak from the LO was measured in the following way: the LO current through the diodes was adjusted to a certain level I_d using a LO frequency of 19.0 MHz. I_d is arbitrarily chosen as a typical drive level. The reading on a μV meter connected to the output of the 19 MHz IF strip was then measured. Then the diodes were disconnected and a current source was connected to the output transformer and the level I_c was raised to give the same reading on the μV meter as in the previous case. The leak was then defined as:

$$\text{Leak} = 20 \log_{10} \frac{I_d}{2I_c} \text{ db.}$$

(An unbalance current ΔI_d will pass through half the primary winding, but I_c will use the full primary winding, therefore $2I_c$ in the denominator.) The leak defined in this way could be varied from 45 to 25 db with the LO potentiometer. The lower level of 25 db is due to the self balancing properties of the circuit, i.e. a third diode will be turned on when the unbalance voltage across the transformer exceeds a certain value.

(4) Third order intermodulation figures were checked for some frequencies under the different conditions and found to be approximately the same level as the second order. In this configuration second order IM should ideally be cancelled so the figures given here are not the true distortion in each diode.

We can also get some cancellation of third order in this configuration by driving the diodes slightly unequally. These cancelling effects will show up if, for example, the IM figure is measured versus drive level. The IM rejection will not always increase steadily versus drive current, but can go through one or more peaks. This can happen both for second and third order products.

(5) One could get the narrow band intermodulation rejection to much better values than presented here by adjusting the LO drive or by putting bias on the diodes. This is due to the above mentioned cancelling effects.

Using trimming capacitors at different points in the ring also improved the performance considerably. As mentioned before, our main interest was in wideband configurations, and solutions that would make it necessary to divide up the frequency band were not considered at this stage of the development.

(6) The heatsinks on the LO transistors were removed and the emitter bias currents in these transistors were reduced to 30 mA, to reduce collector capacities and raise the LO source impedance. Measurements are shown in Table 8. The intermodulation showed no significant dependence on the local oscillator drive impedance.

(7) The following noise measurements were done, see Table 7. The LO potentiometer was adjusted for maximum IM figure for interfering frequencies of 10 MHz and 12 MHz. This relatively bad noise figure, 12-14 db, is certainly due to the high source impedance seen by the output buffer. The noise figure for this buffer amplifier versus source impedance is shown in Figure 14. The output impedance of the mixer is approximately 11 pF in parallel with 6 k ohm at 19 MHz. With this source impedance and the output transformer in addition, the noise figure will almost certainly be $\geq$ 20 db. The available power gain of the input buffer is approximately 200 times (23 db). If we then assume 20 db noise figure in the output buffer, the contribution from this stage to the overall noise figure will be 3 db.

(8) The actual power gain of the input buffer is 10 db. The power loss of the mixer with 100 ohm resistors is approximately 10 db. The current loss in the mixer is approximately 5.5 db. The theoretical minimum value is 3.92 db, found from a simple Fourier series expansion, assuming ideal switches.

(9) The HP 2350 hot-carrier diodes (Schottky-barrier diodes) can be purchased matched for use in mixers (then identified as HP 2374). The general idea behind this configuration was that it should be relatively easy to keep a good balance in the system and only one transformer with relatively narrow band requirements is necessary (the chokes can be replaced by resistors). This circuit is therefore suited for the use of thin-film technology. A circuit designed for this purpose is shown in Figure 15.

A possible advantage of the mixer circuit used in Alouette I and II, is the higher ratio of local oscillator drive current to signal current in the diodes due to the fact that the two conducting diodes are in series for the local oscillator and in parallel for the signal. The two conducting diodes are also forced to have the same local oscillator current. Measurements on both under approximately the same conditions indicate no great improvement in intermodulation by using the circuit in Figure 13, but slightly more broadband IM rejection was obtained.

A third mixer scheme using hot-carrier diodes driven from voltage sources and using a special biasing technique described in reference 14, indicates the possibility of obtaining good narrow band (but temperature sensitive) third order IM rejection. This technique is based on using two hot-carrier diodes in a balanced configuration and biased to different currents to get a cancelling effect of intermodulation caused by the fourth and sixth coefficient in a Taylor expansion of the diode current versus voltage. This configuration was not tested here, but can perhaps be of importance in a receiver design that uses several mixers, and this will be referred to later in the general discussion at the end of this report.

A mixer circuit using four field-effect transistors as switches instead of diodes was tested for two types of transistors, the TI 2N3823 and AMELCO U1551. The circuitry used in these measurements is shown in Figures 16 and 17, and the results are given in Table 9. The results were not too promising and further work in mixers using field-effect transistors was for the time being stopped.

6. PARAMETRIC UP-CONVERTERS

6.1 INTRODUCTION

The possibility of using a parametric upper sideband up-converter was investigated. The power handling capability for a varactor can be very high. In addition, terminating such a converter by a narrow band filter results in a narrow band input signal circuit tunable over a wide range. In the case of series tuned input and output circuits the impedance will be:

$$Z_{in}(j\omega_s) = \frac{1}{j\omega_s C_o} + \frac{k}{\omega_s \left(Z_{out} + R_s + \frac{1}{j\omega_{out} \cdot C_o}\right)} \quad \text{.....(6.1)}$$

$Z_{in}(j\omega_s)$ = input impedance

C_o = equivalent of varactor diode dc capacity (not the static capacity)

k = constant, depending on the diode parameters

Z_{out} = impedance looking into the terminating network from the output port

R_s = diode series loss resistance

We will come back to the above expression later.

Some effort was put into the investigation of such a circuit for use in the sounder. Because of delivery times the preliminary measurements presented in this report were performed using components already available in the laboratory.

6.2 GENERAL THEORY

The theory for up-converters of this type is thoroughly dealt with in the literature, references 5, 17, 19, and here we will only give some of the basic considerations.

The equivalent circuit for a varactor diode is shown in Figure 18, and simplified for the low frequencies involved in the sounder in Figure 19.

If the diode capacity is made time dependent by a so-called pumping signal on a frequency f_p, it is possible to shift and amplify a signal on a frequency f_s to f_o where $f_o = f_s + f_p$. The device used in this way is called an upper sideband up-converter (if $f_p < f_s$). This can be made very stable if properly terminated. The frequencies mentioned, f_s, f_p, f_o are the basic frequencies. In addition one will always have a lower sideband, $f_p - f_s$, that has to be properly terminated. Other frequencies are present to an extent depending on the capacity-voltage relationship and the way the diode is driven.

There are several ways of analyzing a converter, (references 5, 17, and 19). The most straightforward method to establish the main details of the circuit will be the linearized admittance method.

Here the following assumptions are used:

$$C(t) = C_0 + C_1 \cos \omega_p t \qquad \text{.....(6.2)}$$
$$= C_0 (1 + 2 \gamma \cos \omega_p t)$$
$$= C_0 \left[1 + \gamma (e^{j\omega_p t} + e^{-j\omega_p t})\right]$$

C_0, C_1 = real quantities

ω_p = pump frequency

$\gamma = \frac{C_1}{2C_0}$ = relation between the first harmonic of the pumped capacity and the dc-capacity (dynamic)

The following currents and voltages are assumed present:

$$v = v_s e^{j\omega_s t} + V_s^* e^{-j\omega_s t} + V_i e^{j\omega_i t} + V_i^* e^{-j\omega_i t} + V_o e^{j\omega_o t} + V_o^* e^{-j\omega_o t} \qquad \text{....(6.3)}$$

$$i = I_s e^{j\omega_s t} + I_s^* e^{-j\omega_s t} + I_i e^{j\omega_i t} + I_i^* e^{-j\omega_i t} + I_o e^{j\omega_o t} + I_o^* e^{-j\omega_o t} \qquad \text{....(6.4)}$$

$$\omega_s + \omega_i = \omega_p$$
$$\omega_s + \omega_p = \omega_o \qquad \text{....(6.5)}$$

ω_i = lower sideband frequency "idler"

ω_o = upper sideband frequency

ω_s = signal frequency

We will only mention here that all information about the pump circuitry has disappeared in this procedure, and the method can not be used for calculating the overload characteristics and distortion. Using the relation:

$$i = \frac{d}{dt} \left[C(t)\, v(t)\right] \qquad \text{....(6.6)}$$

the following matrix can be set up:

$$\begin{bmatrix} I_i^* \\ I_s \\ I_o \end{bmatrix} = \begin{bmatrix} -j\omega_i C_0 & -j\omega_i \gamma C_0 & 0 \\ j\omega_s \gamma C_0 & j\omega_s C_0 & j\omega_s \gamma C_0 \\ 0 & j\omega_o \gamma C_0 & j\omega_o C_0 \end{bmatrix} \begin{bmatrix} V_i^* \\ V_s \\ V_o \end{bmatrix} \qquad \text{....(6.7)}$$

In an upper sideband up-converter $V_i^* = 0$. Then:

$$\begin{bmatrix} I_s \\ I_o \end{bmatrix} = \begin{bmatrix} j\omega_s C_0 & j\omega_s \gamma C_0 \\ j\omega_o \gamma C_0 & j\omega_o C_0 \end{bmatrix} \begin{bmatrix} V_s \\ V_o \end{bmatrix} \qquad \text{....(6.8)}$$

This is then the relation for the signal currents and voltages of the frequencies of interest assuming the idler-frequency is shorted. It can be shown, reference 5, that a slightly different matrix will appear if the idler current is zero.

As long as the idler has a reactive termination the equations (6.8) can be used as a good approximation. If the idler has a termination that is slightly resistive, the gain will drop drastically.

The theoretical maximum power-gain is according to the Manley-Rowe relations, given by:

$$G_{p_{max}} = \frac{f_o}{f_s} \qquad \ldots.(6.9)$$

The circuit for further analysis is shown in Figure 20. The two parallel resonant circuits on f_s and f_o are put there to symbolically express the necessary filtering. In practice it will be done differently. R_1 and R_0 are losses, R_s is diode loss, L_s and L_o are present to tune out the reactive part of the input and output impedances.

To simplify the calculations, the matrix (6.8) has to be inverted and we find:

$$\begin{bmatrix} V_s \\ V_o \end{bmatrix} = \begin{bmatrix} \frac{1}{j\omega_s C_o'} & -\frac{\gamma'}{j\omega_o C_o'} \\ -\frac{\gamma'}{j\omega_s C_o'} & \frac{1}{j\omega_o C_o'} \end{bmatrix} \begin{bmatrix} I_s \\ I_o \end{bmatrix} \qquad \ldots.(6.10)$$

where to a very good approximation both for an open circuited and short circuited idler (reference 5 page 39):

$$\gamma' = \gamma$$
$$C_o' = C_o \qquad \ldots.(6.11)$$

Equation (6.10) can also be written:

$$\begin{bmatrix} V_s \\ V_o \end{bmatrix} = \begin{bmatrix} Z_{11} & Z_{12} \\ Z_{21} & Z_{22} \end{bmatrix} \begin{bmatrix} I_s \\ I_o \end{bmatrix} \qquad \ldots.(6.12)$$

and the diode-resistance R_s can be directly added to Z_{11} and Z_{22}. From here on the calculation of gain, input and output impedances, etc. are straightforward and the details can be found, for example, in references 5, 17, 19. We will only give the results here.

The transducer gain can be expressed in the following form assuming resonance in both input and output circuits:

$$G_t = \frac{4\ R_g R_\ell\ \gamma^2}{(\omega_s C_0)^2} \cdot \frac{1}{\left[(R_g + R_1 + R_s)(R_\ell + R_o + R_s) + \frac{\gamma^2}{\omega_s \omega_o C_0^2}\right]^2} \quad \ldots\ldots(6.13)$$

G_t has a maximum value for $R_g = R_\ell$ assuming the total losses are the same at input and output, i.e. $R_1 + R_s = R_o + R_s = R$.

This value of R_g is:

$$R_g = R_\ell = R\sqrt{1 + \frac{\gamma^2}{\omega_s \omega_o C_0^2 R^2}} \quad \ldots\ldots(6.14)$$

$$R_g \approx \sqrt{\omega_s \omega_o C_0} \quad \text{for} \quad \frac{\gamma^2}{\omega_s \omega_o C_0^2 R^2} \gg 1 \quad \ldots\ldots(6.15)$$

The input impedance, Z'_{in}, is given by:

$$Z'_{in} = \frac{1}{j\omega_s C_0} + \frac{\gamma^2}{\omega_s \omega_o C_0^2 \left(\frac{1}{j\omega_o C_0} + R_\ell + R_s + R_o + j\omega_o L_0\right)} \quad \ldots\ldots(6.16)$$

Z'_{in} differs from Z_{in} (see Figure 20) in that R_s in (6.16) is assumed pulled out into the input and output circuits.

At resonance Z'_{in} will be equal to R'_{in} given by:

$$R'_{in} = \frac{\gamma^2}{\omega_s \omega_o C_0^2 (R_\ell + R_o + R_s)} \quad \ldots\ldots(6.17)$$

Assuming losses in the output circuit negligible compared with R_ℓ:

$$R'_{in} = \frac{\gamma^2}{\omega_s \omega_o C_0^2 R_\ell} \quad \ldots\ldots(6.18)$$

Similarly

$$R'_{out} = \frac{\gamma^2}{\omega_s \omega_o C_0^2 (R_g + R_1 + R_s)} \quad \ldots\ldots(6.19)$$

or if $R_g \gg R_1 + R_s$

$$R'_{out} = \frac{\gamma^2}{\omega_s \omega_o C_o^2 R_g} \qquad \ldots.(6.20)$$

γ is a parameter that depends on drive level and the diode voltage-capacity characteristic. In reference 5 pages 127-219 values of C_o and γ are listed vs drive level for abrupt junction diodes and graded junction diodes.

6.3 NOISE

Assuming the major contribution to the noise in a parametric up-converter is coming from the thermal noise in the circuit losses, and that the shot noise is insignificant, it is then possible to calculate the noise factor using the equivalent circuit shown in Figure 21. This assumption can be justified from the literature, reference 5. Here C_a is inserted in order to consider the general case of a highly capacitive antenna. This equivalent can then be further simplified as shown in Figure 22 where:

$$Z'_{11} = \frac{1}{j\omega_s C_o} + R_g + R_1 + R_s + j\omega_s L_s + \frac{1}{j\omega_s C_a}$$

$$Z'_{22} = \frac{1}{j\omega_o C_o} + R_\ell + R_o + R_s + j\omega_o L_o$$

Then the following matrix equation will be considered:

$$\begin{bmatrix} e_{ns} \\ e_{no} \end{bmatrix} = \begin{bmatrix} Z'_{11} & Z_{12} \\ Z_{21} & Z'_{22} \end{bmatrix} \begin{bmatrix} i_{ns} \\ i_{no} \end{bmatrix} \qquad \ldots.(6.21)$$

where e_{ns} and e_{no} are as given in Figure 21.

Putting $e_{no} = 0$ will give us the noise current i'_{no} due to e_{ns} and then also the delivered noise power P_1 to R_ℓ

$$i'_{no} = \frac{e_{ns}}{Z_{12} - \dfrac{Z_{11}' \cdot Z_{22}'}{Z_{21}}} \qquad \ldots.(6.22)$$

and

$$P_1 = \frac{e_{ns}^2 \left|Z_{21}\right|^2 R_\ell}{\left|Z_{11} \cdot Z_{21} - Z_{11}' \cdot Z_{22}'\right|^2} \qquad \ldots.(6.23)$$

Putting $e_{ns} = 0$ gives us i_{no} due to e_{no}:

$$i_{no} = \frac{e_{no}}{\left| Z_{22}' - \frac{Z_{21} \cdot Z_{12}}{Z_{11}'} \right|^2} \qquad \ldots.(6.24)$$

and delivered noise-power P_2 is given by

$$P_2 = \frac{e_{no}^2 \left| Z_{11}' \right|^2 R_\ell}{\left| Z_{22}' \cdot Z_{11}' - Z_{21} \cdot Z_{12} \right|^2} \qquad \ldots.(6.25)$$

The noise figure is then:

$$NF = \frac{P_1 + P_2}{P_1'} \qquad \ldots.(6.26)$$

Where:

$$P_1' = P_1 \frac{T_o R_g}{T_o R_g + T_d R_s + T R_1} \qquad \ldots.(6.27)$$

Using the values for the Z's, e_{ns} and e_{no} gives the following expression after simplification:

$$NF = 1 + \frac{T_d \cdot R_s + T R_1}{T_o R_g} + \left(\frac{\omega_s C_o}{\gamma}\right)^2 \left(\frac{T_d \cdot R_s + T R_o}{T_o \cdot R_g}\right) \left| R_g + R_1 + R_s + j\left[(\omega_s L_s - \frac{1}{\omega_s}\left(\frac{1}{C_a} + \frac{1}{C_o}\right)\right] \right|^2 \qquad \ldots.(6.28)$$

Before proceeding further we assume all temperatures equal to T_o to simplify the expression

$$NF = 1 + \frac{R_s + R_1}{R_g} + \left(\frac{\omega_s C_o}{\gamma}\right)^2 \left(\frac{R_s + R_o}{R_g}\right) \left[\left(R_g + R_1 + R_s\right)^2 + \left(\omega_s L_s - \frac{1}{\omega_s}\left(\frac{1}{C_a} + \frac{1}{C_o}\right)\right)^2 \right] \qquad \ldots.(6.29)$$

Under normal conditions the input circuit is in resonance:

$$NF = 1 + \frac{R_s + R_1}{R_g} \left(\frac{\omega_s C_o}{\gamma}\right)^2 \left(\frac{R_s + R_o}{R_g}\right) \left(R_g + R_1 + R_s\right)^2 \quad \ldots.(6.30)$$

In this case the value of R_g giving best noise figure is equal to:

$$R_g \approx \frac{\gamma}{\omega_s C_o} \times \sqrt{\frac{R_s + R_1}{R_s + R_o}} \quad \ldots.(6.31)$$

Assuming $L_s = 0$ and $C_a = \infty$

$$NF \approx 1 + \frac{R_1 + R_s}{R_g} + \frac{R_o + R_s}{R_g \cdot \gamma^2} \quad \ldots.(6.32)$$

Assuming $L_s = 0$ and $C_a \neq \infty$

and $(\omega_s C_o)^2 (R_g + R_1 + R_s)^2 \ll 1$

$$NF \approx \frac{R_o + R_s}{R_g \cdot \gamma^2} \left(1 + \frac{C_o}{C_a}\right)^2 \quad \ldots.(6.33)$$

Here is also assumed that R_g is of less or the same order as the losses.

Assuming a transformer (1 : n) on the input

$$NF \approx \frac{R_o + R_s}{R_g n^2 \gamma^2} \left(1 + \frac{C_o}{C_a} n^2\right)^2 \quad \ldots.(6.34)$$

From this:

$$n_{opt} = \sqrt{\frac{C_s}{C_o}} \quad \ldots.(6.35)$$

$$\text{and } NF_{opt} = \frac{4(R_o + R_s) C_o}{\gamma^2 \cdot R_g \cdot C_a} \quad \ldots.(6.36)$$

Therefore

$$NF_{opt} \propto \frac{1}{R_g \cdot C_a} \quad \ldots.(6.37)$$

if the transformer turns ratio is given by equation (6.35).

For the 240' dipole antenna used in Alouette II, $R_g = .1\Omega$, and $C_a = 120$ pF at 100 kHz and assuming free space conditions. If we further assume $R_o = 10\Omega$, $R_s \ll R_o$, $\gamma = 1/3$ and $C_o = C_a$ we get:

$$F_{min} = 36 \text{ db} \qquad \ldots.(6.38)$$

It will easily be seen here that tuning out antenna and diode capacities by the series choke gives a very narrow band, high Q, input circuit. The reason is that to avoid too much reduction in available gain the load impedance has to be high and the resistive part of the input impedance is therefore low. The resistive loss in the choke will in this case also control the noise figure for the parametric up-converter itself.

The available gain, G_{av_1}, has to be kept above a certain minimum value which depends on the noise figure of the amplifier following the parametric up-converter. The noise figure for the cascaded system is given by:

$$NF_{12} = NF_1 + \frac{NF_2 - 1}{G_{av_1}} \qquad \ldots.(6.39)$$

The available gain, G_{av_1}, can easily, under these working conditions be a large loss, and the noise figure can be entirely controlled by the second term in 6.39.

6.4 BANDWIDTH

An extensive study of the ultimate bandwidth limits for parametric up-converters is carried out in reference 18, pages 111 - 128. From these considerations bandwidths of 10 : 1 are relatively easy to obtain, under normal working impedances, if some sacrifice in gain is allowed.

In practice pump leak and distortion problems will probably be limiting factors. We will come back to these considerations in the general discussion of the system.

As mentioned in 6.2 the linearized admittance method gives little information about distortion from saturation effects and non-linearities.

A special case is relatively easy to analyze more exactly, i.e. the current pumped abrupt junction diode, references 20, 21. In all other cases the exact calculation is extremely difficult to carry out, mainly because the diode is not a pure capacity (it has at least a resistance in series) and a non-abrupt diode gives an infinite series for the pumped capacity. The diode used in the measurements to be presented here has a capacity voltage slope very close to that of an abrupt junction varactor. According to reference 21 an up-converter using such a diode will have no 2nd and 3rd order intermodulation from non-linearities, but the saturation effect will cause distortion. It is

shown (21) that the gain of the up-converter is a function of the input current, i.e. the output current can be expressed as a power series of the input current. From this expression the intermodulation is found directly. The 3rd order intermodulation is shown in Figure 23 versus P_o/P_{om} where P_o is the output power and P_{om} is the maximum output power. We will come back to Figure 23 when discussing the experimental results.

6.5 EXPERIMENTAL RESULTS

As mentioned before, components available in the laboratory were used for the preliminary measurements covered in this report. The diode used was 1N5148 (Motorola) because of its high breakdown voltage, large power handling capacity, low losses and because it has a capacity-voltage characteristic close to that of an abrupt junction. An Alouette II 19 MHz IF amplifier and crystal filter were used for amplifying and filtering the upper sideband.

To reduce leak from the high level pump source a balanced pump circuit was used, and is shown in Figure 24 both for current and voltage pumping. This arrangement of the pumping circuit makes it very convenient to tune the circuit separately without affecting the tuning of the input and output circuits. When the pump circuit is tuned properly and made broad enough to cover the LO frequency range, the input and output circuits can be simply tuned up by series inductors and suitable matching networks. A small capacity can be inserted in series in the output circuit to avoid shunting the input frequencies and to terminate the lower sideband reactively.

An additional advantage of using a balanced pump circuit is the ability to stabilize it without affecting the input and output circuits too much. Whatever you put between "the hot sides" of the diodes will not be seen from the input and output ports.

Several circuits were designed covering different frequency ranges and both current pumping and voltage pumping were used.

Going from voltage pumping to current pumping did not improve intermodulation significantly. This result should indicate that the intermodulation in these cases primarily has its origin in saturation effects. In addition, the voltage pumping scheme was much easier to implement, balance and stabilize.

It was necessary in the measurements to concentrate on the low frequency range in order to be able to obtain any gain using 19 MHz as output frequency.

The circuit presented in Figure 25 had the following characteristics:

Tangential sensitivity $\leq .05$ μV into 50 Ω (5 kHz bandwidth centred on 800 kHz).

Noise figure at 800 kHz ≤ 2.7 db.

Dynamic range ≈ 141 db (equals 0.6V at the input).

Intermodulation (2nd and 3rd) approximately 80 db without tuning (5 kHz bandwidth) and rebalancing for each frequency combination (IM above 1 μV).

The output voltage with a constant voltage in series with 50 ohms on the input is given versus frequency in Figure 26. The dc bias voltages on the diodes were ± 20V and the diodes were driven fully. R_g was 50 ohms. The signal input circuit was tuned for 800 kHz and the output for 18.9 MHz (in this case a crystal filter with 18.9 MHz center-frequency and 120 kHz bandwidth was used with insertion loss less than 6 db).

Assuming that all intermodulation is coming from saturation effects of the type discussed in reference 21, we can get a rough idea of the intermodulation level we should expect to have.

If we do not include the filtering properties of the up-converter, the intermodulation level according to our definition should be (3rd order):

$$IM = 10 \log \left(\frac{P_{om} \cdot (10)}{P_{ref} \cdot G} \right)^{2/3}$$

P_{om} = maximum output power from the up-converter

P_{ref} = the reference power level on the input of the up-converter

G = small signal gain of the up-converter

In the experimental up-converter mentioned above the maximum output power was measured at approximately 150 mW. The gain was close to 20 times for 800 kHz (the frequency used in the IM measurements i.e. f_o). Using 1 μV into 50 ohms as the reference input level, we should have an intermodulation rejection of approximately 84 db. In addition to this rejection by the diodes themselves, the filtering properties of the up-converter on the interfering frequencies will increase this figure.

Another up-converter covering the signal band 2.5 to 4.5 MHz and output frequency of 19 MHz was measured. Because of the low available gain the noise figure measurement using ε 50 ohm source impedance (matched) was strongly affected by the circuitry following the converter. Intermodulation measurements are shown in Table 10. In the 3rd order IM figures the filtering effect is easily seen. According to (6.40) the 3rd order IM should be equal to approximately 87 db.

Generally we can then say, assuming that saturation effects cause the intermodulation, that the requirements for getting good intermodulation rejection will be:

(1) High pump level (because $P_{om} \propto P_{pump}$) and this requires diodes with high breakdown voltage and high minimum capacity (21).

(2) Use low gain in the converter (which in turn increases the noise figure).

(3) Use a crystal filter on the output that (together with its matching network) gives a highly selective input.

A third up-converter tuned to 300 kHz and using lower drive level ($V_{bias} = \pm 7V$) was designed. The following measurements were done on this circuit that had 50 ohms input impedance using a step-up transformer.

Noise figure at 100 kHz with source impedance equal to the actual free space antenna impedance of a 240' dipole (see Figure 1) is 64 db. The input impedance was 50 ohms using a step-up transformer 1:4.7. The transformer was taken out and the noise figure was measured using a source impedance 2.2 ohms and no series capacity. The noise figure was then 30 db. The noise figure at 300 kHz using the actual antenna impedance was 52 db.

The noise figure for this circuit using the proper 50 ohm source impedance was approximately 2 db on 300 kHz. In addition to the circuits mentioned here other circuits were designed and they were showing the same typical characteristics as mentioned before.

7. GENERAL SYSTEM CONSIDERATIONS

It can be concluded from the previous considerations that there are two areas where the parametric up-converter can have certain advantages over other system solutions.

(1) For the very low frequencies where the antenna is quite reactive and where, because of high mismatch losses, intermodulation rejection is of small importance but noise figure is of great importance.

(2) For the upper frequencies where antenna efficiency is much higher, noise figure becomes a secondary consideration. Due to strong interference from solar noise bursts, and HF signals from ground based transmitters penetrating the ionosphere, high intermodulation rejection is required to avoid generation of spurious signals within the receiving system.

Let us consider (1) first. In Figure 27 the equivalent noise temperature on the antenna source resistance is plotted versus frequency for different front ends for the 240' dipole source impedance. Here the noise figure of the following stages is assumed equal to 0 db. As mentioned before, the large mismatch losses due to the high capacitive reactance of the antenna will in most cases be the controlling factor for the noise figure together with the noise figure in the stages following the front amplifier (or converter) i.e. $\frac{F_2 - 1}{G_1}$ will be the largest term in the expression for the noise figure. The up-converter equivalent noise temperature has been calculated assuming an untuned signal circuit and a direct coupling to the antenna (without a transformer). The input capacity has also been assumed equal to the antenna capacity. The loss in the output circuit is the parameter shown in the Figure 27.

The solution for the low frequencies using an up-converter can be to use it as the first stage, or the up-converter can directly follow a field-effect transistor buffer. The up-converter used in the first mentioned manner will then have a wideband low pass input where the diode capacity will be one of the low pass filter shunt elements. The filter must have a cutoff frequency $\approx$2 MHz. The pump power must be low because of difficulties with LO leakage when the pump frequencies are so close to the IF. The idler termination can cause difficulties when going down to 10 kHz which is the present goal for ISIS-C. Leak and filter problems will obviously be the main problems using the up-converter in this way. Secondly one has to rely upon a low noise second stage.

The idea of using the up-converter after a field-effect buffer will now be briefly explained. The field-effect amplifier will not be affected by the antenna series capacity as long as the input impedance is kept high, see Figure 27. It has therefore a relatively good noise figure and broadband characteristics working from the highly reactive antenna. The up-converter following this buffer can then work from a "normal" source impedance and will therefore have very low noise figure compared to resistive mixers. The overall noise figure will then be minimized. The main objection against this system is due to the difficulties involved in adding a low-pass filter between the antenna and the input to the field-effect transistor. Using a filter in front of the FET will ruin the noise figure or make the antenna circuit narrow band. If the filter is removed the field-effect transistor must operate in the presence of wideband high-level interference from the antenna. Third order intermodulation rejection is very good in a field-effect transistor but because of its square law transfer characteristic second order IM is bad. Some sort of a balanced system could perhaps reduce second order intermodulation products to acceptable levels. In practice critical circuit adjustments and tracking of transistor characteristics would probably be required.

For the higher frequencies where intermodulation rejection is of great importance, the parametric amplifier could perhaps have some advantages over resistive mixers. The reason is that it should have relatively broadband IM rejection if the assumption that intermodulation is coming from saturation effects is true. Then the intermodulation rejection will be directly related to the pump level and this can be increased considerably over the levels used in the preliminary tests in the laboratory. Filtering for leak is no problem because of the wide separation of the IF and the pump frequencies. To get sufficient gain to overcome the noise figure of the next stage for the upper frequencies an IF around 100 MHz should be used. That is well within the state of the art for crystal filters. The crystal filter input characteristics together with its matching network must give the input port the characteristics of a narrow band filter.

Generally it can be stated that solving all the problems for the different frequency ranges in ISIS-C is impossible in a single system. It seems to be necessary to divide the total frequency band up into octave bands, with prefiltering to reduce second order intermodulation and then use switched front ends designed especially and matched for the different bands. For some of these bands it should be sufficient only to switch the filters and compensating elements.

In using such a system with multiple bands, the hot-carrier diode mixers can be of great value. As mentioned before they have narrow band properties much better than the broad band performance described earlier in this report.

The Alouette I and II mixers had not as good broadband characteristics as the one described in detail in this report, but good narrow-band figures were easier to obtain in those mixers. The scheme used in Alouette II can therefore not be excluded.

In addition the balanced hot-carrier diode mixer mentioned in reference 14 should, according to the data sheets, have very good narrow-band intermodulation rejection because of the cancellation of third order products which is quite unusual in a balanced circuit. Unfortunately that type of mixer is very temperature sensitive but this problem can be overcome.

8. REFERENCES

1. T.R. Hartz: A Study of Interference on the Alouette Topside Sounder Records. DRTE Report No. 1123.

2. H. Kowalik: Report or Memorandum in preparation.

3. C.A. Franklin, R.J. Bibby, R.F. Sturrock, D.F. Page: Electronic and System Design of the Canadian Ionospheric Satellite. DRTE Report No. 1158.

4. C.A. Franklin, M.A. Maclean: The Alouette II Topside Ionospheric Sounder. Paper presented at the International Conference on Electronics and Space, April 10-15, 1967, Paris.

5. L.A. Blackwell and K.L. Kotzebue: Semiconductor Diode Parametric Amplifiers Book, Prentice-Hall, Inc., Englewood Cliffs, N.J. 1961.

6. D.G. Tucker: Intermodulation Distortion in Rectifier Modulators. Wireless Engineer Vol. 21, June 1954.

7. D.P. Howson: The Relative Magnitudes of Modulation Products in Rectifier Modulators and Some Effects of Feedback. Journal Brit. I.R.E. March 1961.

8. D.G. Tucker: Some Aspects of the Design of Balanced Rectifier Modulators for Precision Applications. J. Instn. Electr. Eng. Vol. 95 May 1948.

9. D.G. Tucker: Elimination of Even-order Modulation in Rectifier Modulators. Journal Brit. I.R.E., Feb. 1961.

10. L.M. Orloff: Intermodulation Analysis of Crystal Mixer. Proc. I.E.E. Feb. 1964.

11. R. Nitzberg: Spurious Frequency Rejection. Proc. I.E.E.E. Transactions on Electromagnetic Compatibility. Jan. 1964.

12. L. Von Christiansen: Uber die kubischen verzerrungen am ringmodulator. Frequenz Bd. 5, No. 11/12, 1951.

13. D.G. Tucker: Circuits with Periodically Varying Parameters including Modulators and Parametric Amplifiers. Princeton, N.J., Van Nostrand 1964.

14. A.M. Cowley, F.H. Lepoff: Improved Intermodulation Rejection in Mixers. Hewlett-Packard Journal, April 1967.

15. V. Belevitch: Nonlinear effects in ring modulators. Wireless Engineer, Vol. 26, May 1949.

16. D.G. Tucker, E. Feynes: Nonlinear Effects in Rectifier Modulators. Wireless Engineer, Vol. 27, Feb. 1950.

17. R.P. Rafuse, P. Penfield: Varactor Applications. Book. The M.I.T. Press 1962.

18. P.O. Scheibe: Theoretical Bandwidth Limitations in UHF Parametric Amplifiers and Converters. Stanford Electronics Lab. Technical Report No. 2253-1. Prepared under Office of Naval Research Contract Nonr 225(24) NR 373360.

19. D. Leenov: Gain and Noise Figure of a Variable Capacitance Up-Converter. The Bell Syst. Tech. Journal July 1958.

20. B.S. Perlman: Current Pumped Abrupt Junction Varactor Power Frequency Converters. I.E.E.E. Transactions M.T.T. 13, No. 2, March 1965.

21. S.M. Perlow, B.S. Perlman: A Large Signal Analysis Leading to Intermodulation Distortion Prediction in Abrupt Junction Varactor Up-Converters. I.E.E.E. Transactions, M.T.T. 13, No. 6, November 1965.

22. D.P. Howson, D.G. Tucker: Rectifier Modulators with Frequency Selective Terminations. Proc. I.E.E. Vol. 107, Part B, 1960.

23. T.R. Hartz: DRTE Report in preparation.

24. L. Becker, R.L. Ernst: Nonlinear Admittance Mixers. RCA Review, Dec. 1964.

9. ACKNOWLEDGEMENTS

The author wishes to acknowledge the advice and assistance received from Dr. Colin Franklin and other members of the Space Electronics Section, DRTE. A special thanks to Mr. Robert Hahn who has done all the measurements described in this report and also designed some of the circuits.

APPENDIX A

ANTENNA TEMPERATURE AND SENSITIVITY

Brightness defined as:

$$b = \lim_{\Delta\Omega \to 0} \frac{\Delta S}{\Delta\Omega} \qquad (A.1)$$

ΔS = flux power density per unit area and unit frequency $\left[W \cdot M^{-2} \cdot Hz^{-1} \text{ steradian}^{-1}\right]$.

$\Delta\Omega$ = incremental solid angle subtended by the source at the point of observation.

Using the Rayleigh-Jeans approximation to Planck's law for radiation from a black body we have:

$$b_1 = \frac{2.k.T}{\lambda^2} \qquad (A.2)$$

T = the temperature in degrees Kelvin

λ = radiation wavelength

k = Boltzmann's factor

Brightness temperature can now be defined using this expression.

The brightness temperature of a noise source is defined as the temperature in degrees kelvin of a black body put in the place of the noise source and giving the same radiation.

Therefore

$$T_b = b \cdot \lambda^2 \cdot \frac{1}{2.k} \qquad (A.3)$$

T_b = brightness temperature

Received noise under matched antenna conditions will then be:

$$W_r = \frac{1}{2} \cdot b \cdot \Delta f \cdot \int_{4\pi} A_\Omega \cdot d\Omega \qquad (A.4)$$

It is assumed constant brightness (b) in all directions

Δf = frequency bandwidth

A_Ω = antenna effective area in the direction given by the incremental solid angle $d\Omega$.

The factor of one half allows for random polarization of the noise.

From (A.4):

$$W_r = \frac{1}{2} \cdot \frac{2 \cdot T_b \cdot k}{\lambda^2} \cdot \Delta f \cdot \lambda^2 \int_{4\pi} \frac{g}{4\pi} \, d\Omega$$

$$= k \cdot T_b \cdot \Delta f \cdot \int_{4\pi} \frac{g}{4\pi} \, d\Omega \qquad (A.5)$$

It can be proven that the integral is equal to one.

Therefore:

$$W_r = k \cdot T_b \cdot \Delta f \qquad (A.6)$$

Antenna temperature is then (ideal antenna and no other noise appearing on the antenna terminals)

$$\underline{T_a = T_b} \qquad (A.7)$$

If the noise source only covers a solid angle Ω around the maximum gain direction, the antenna temperature will be:

$$T_a = T_b \cdot \frac{\Omega}{\Omega_1} \qquad (A.8)$$

(Ω_1 is the effective antenna beam angle). For several noise sources we have:

$$T_a = \sum_{n=1}^{n} \frac{b_n \cdot A_n \cdot \Delta\Omega n \cdot \lambda^2}{2 \cdot k} \qquad (A.9)$$

b_n = brightness in the direction of the incremental angle $\Delta\Omega_n$ and effective area of A_n

The factor of 2 in the denominator allows for random polarization.

Operating or system noise temperature is defined as follows:

$$T_{op} = T_o(F-1) + T_a \qquad (A.10)$$

$T_o = 290\ ^\circ k$

F = the noise factor of the receiver

T_a = antenna temperature

$T_o(F-1)$ is also called effective input noise temperature (T_e).

$$T_{op} = T_e + T_a \qquad \text{(A.11)}$$

Brightness or sky temperatures deduced from measurements obtained by Alouette I and II are shown in Figure 28 (See ref. 23).

APPENDIX B

ANTENNA EQUATIONS

A receiving antenna can be presented by the equivalent circuit shown in Figure 29. Here

$$V_a = I_1 \cdot Z_{21} \tag{B.1}$$

I_1 = transmitting antenna equivalent current

Z_{21} = transfer impedance between the two antennas

V_a can also be expressed in this way (V_a and I_1 in rms values):

$$V_a = I_1 \cdot Z_{21} = \sqrt{4 \cdot R_{22} \cdot A \cdot P_{av}} \tag{B.2}$$

where $R_{22} = R_e(Z_{22})$

A = effective antenna aperture with matched load

P_{av} = Poynting vector at the receiving antenna

Received power is then generally:

$$W_r = \frac{4 R_{22} \cdot A \cdot P_{av}}{|Z_{22} + Z_L|^2} R_e(Z_L)$$

$$= A \left(4 R_{22} \frac{R_e(Z_L)}{|Z_{22} + Z_L|^2} \right) P_{av}$$

$$= A' \cdot P_{av} \tag{B.3}$$

A' = effective antenna aperture taking into account the mismatch between the antenna termination and the load.

The relation between gain and effective aperture is:

$$g = A \cdot \frac{4\pi}{\lambda^2} \tag{B.4}$$

Receiver power under matched conditions on both transmitter and receiver is given by:

$$W_r = \frac{g_r \cdot g_t \cdot \lambda^2}{(4\pi r)^2} \cdot W_t = \frac{A_r \cdot A_t}{\lambda^2 r^2} \cdot W_t \qquad \text{(B.5)}$$

r = distance between transmitter and receiver

W_r = power received

W_t = power transmitted

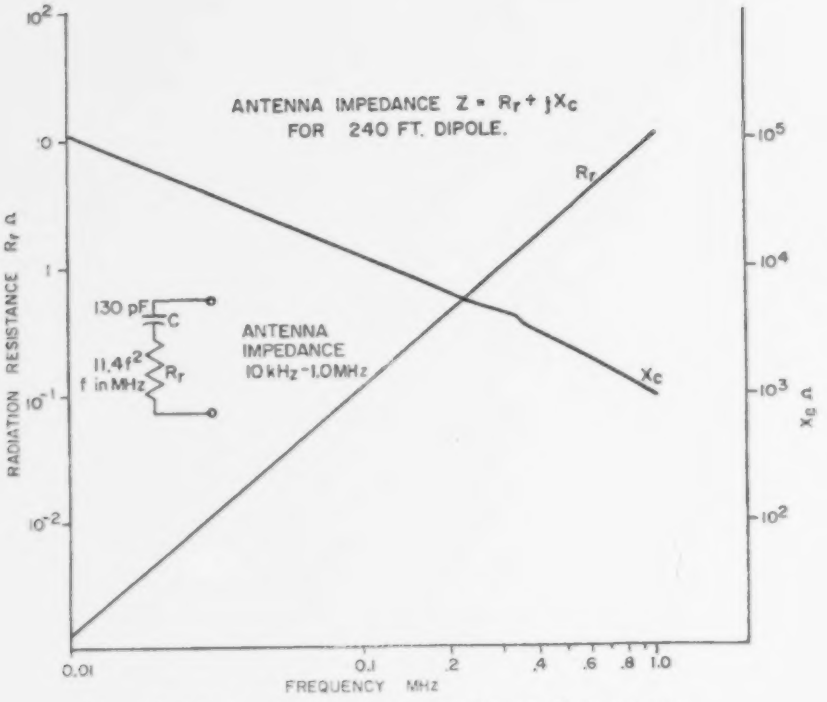

Fig. 1. Antenna impedance versus frequency.

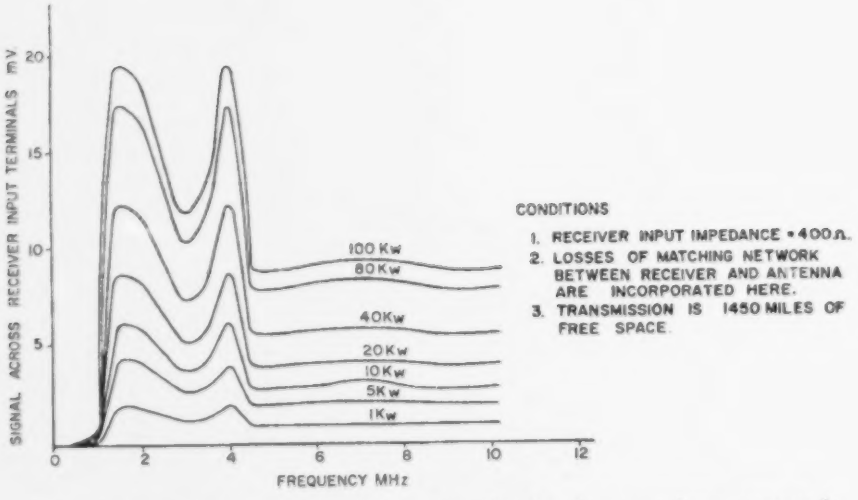

Fig. 2. Signal strength at receiver terminals for various ground transmitter powers.

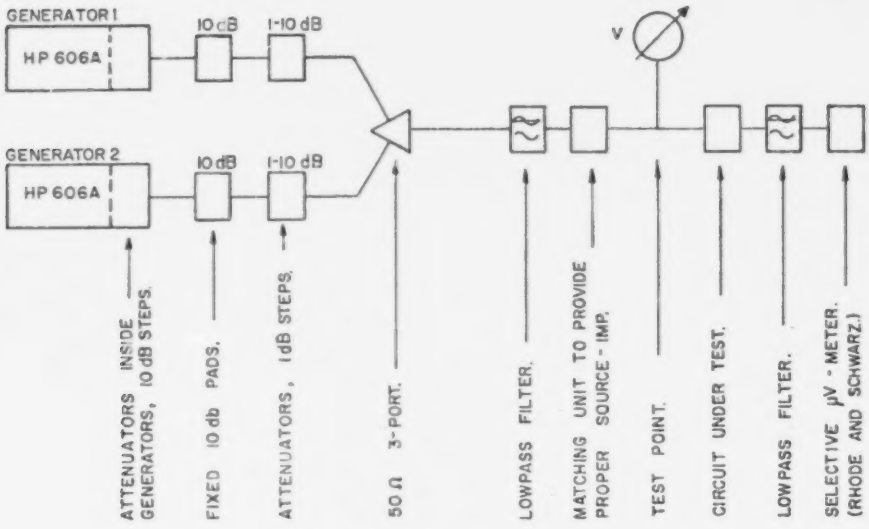

Fig. 3. Test setup for intermodulation checks.

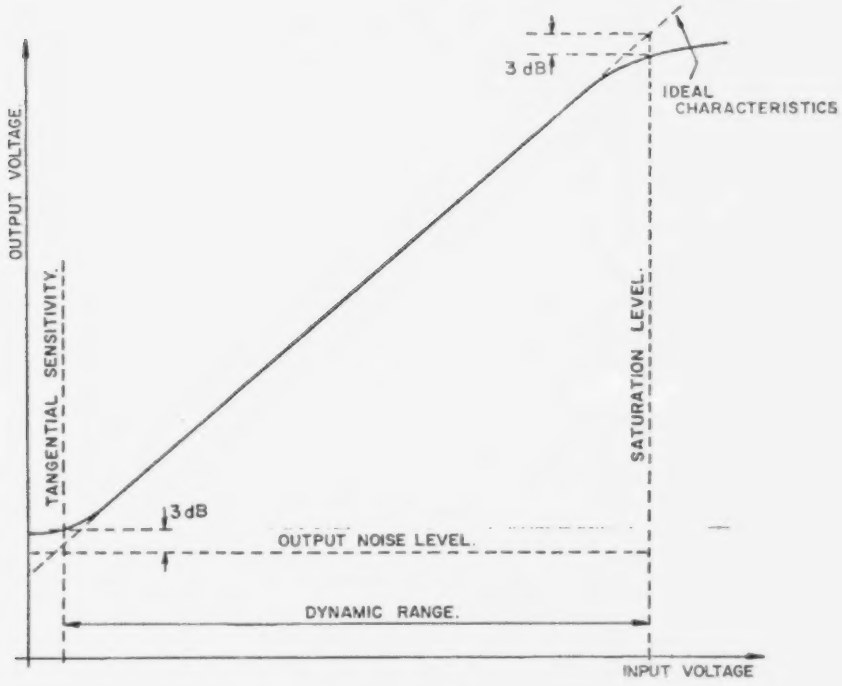

Fig. 4. Typical input-output characteristics.

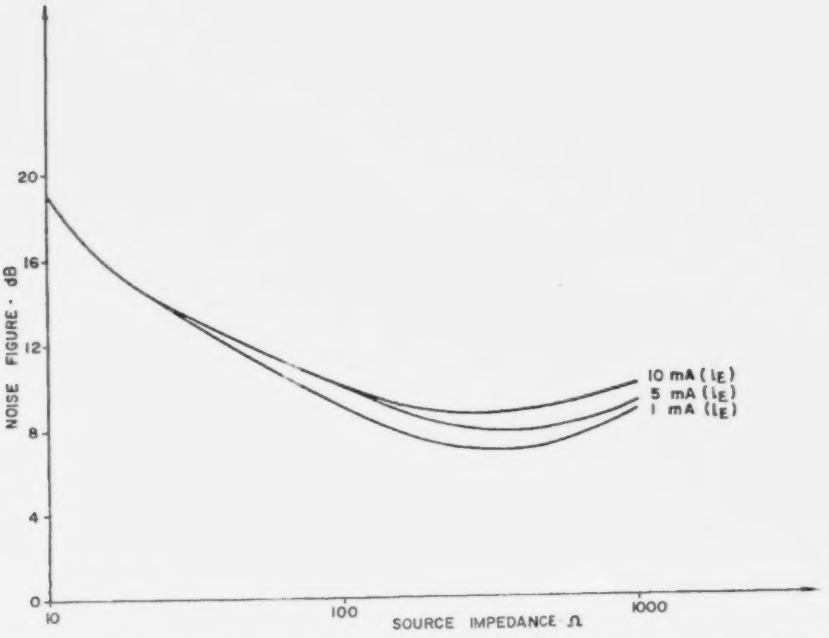

Fig. 5. Noise figure versus source impedance for common base amplifier.

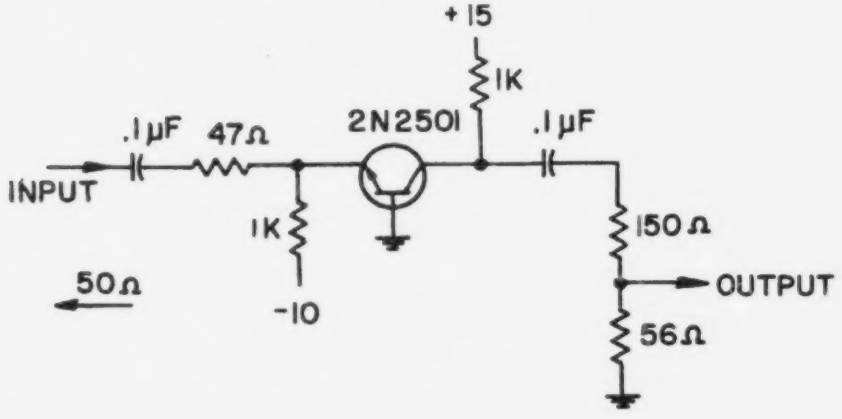

Fig. 6. Single ended common base amplifier.

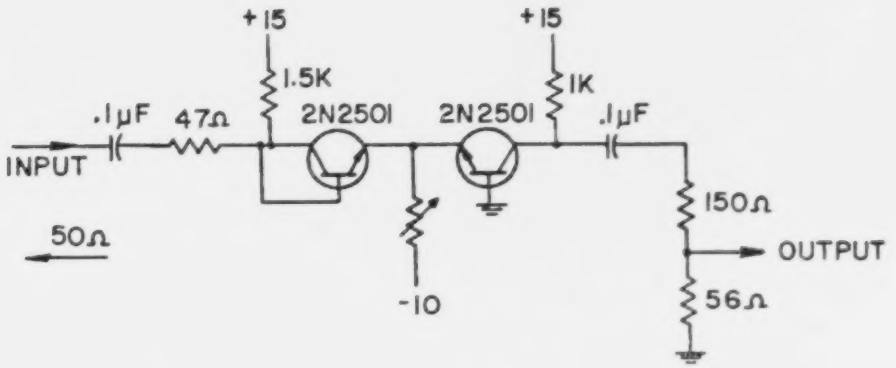

Fig. 7. Single ended common base amplifier with diode compensation.

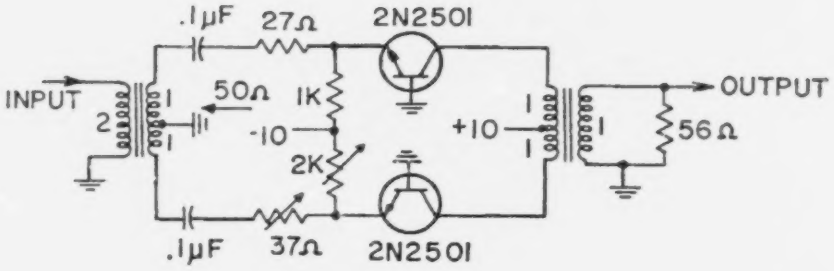

Fig. 8. Push pull common base amplifier.

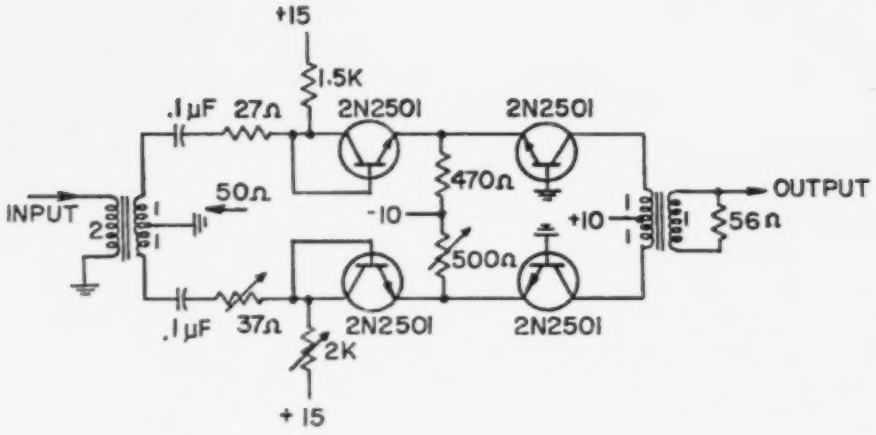

Fig. 9. Push pull common base amplifier with diode compensation.

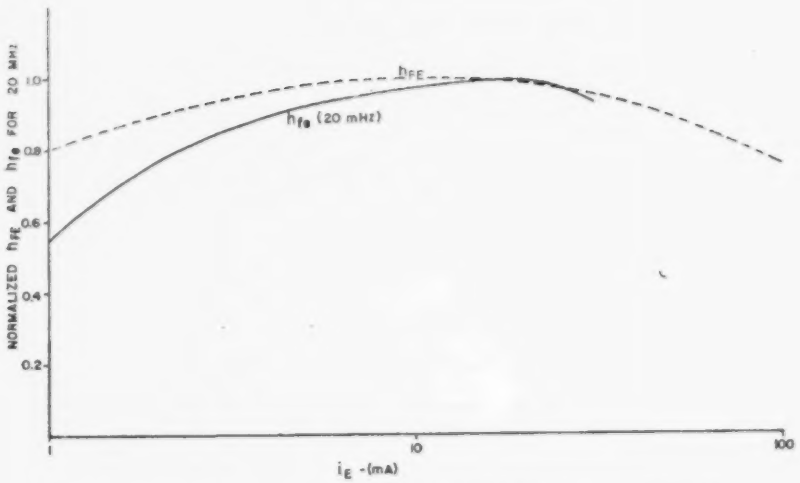

Fig. 10. Current gain for 2N2501 (normalized).

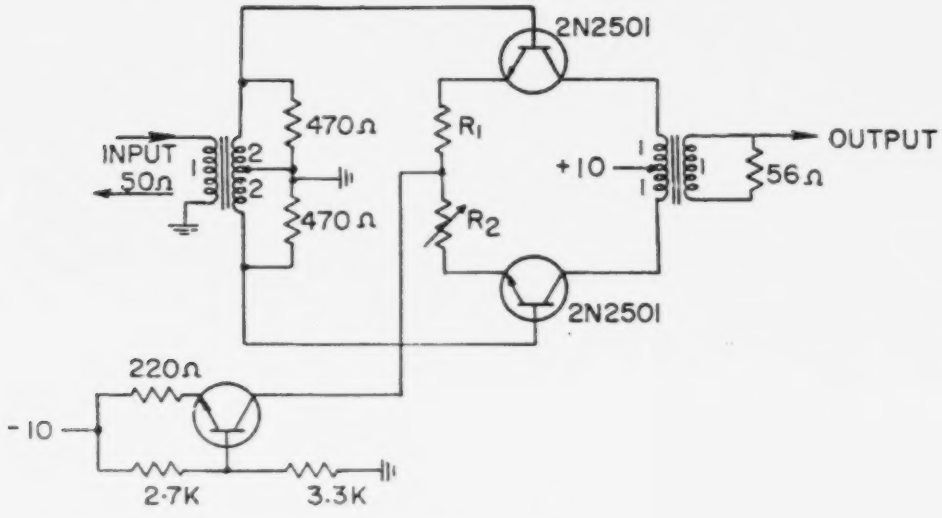

Fig. 11. Differential amplifier.

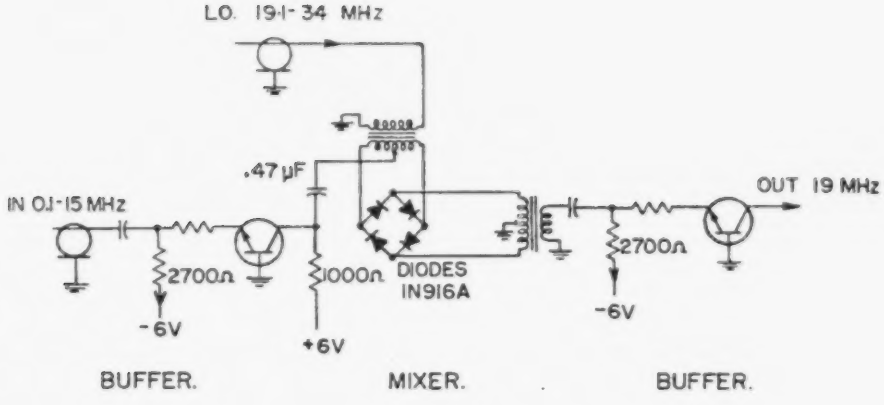

Fig. 12. Balanced wideband mixer.

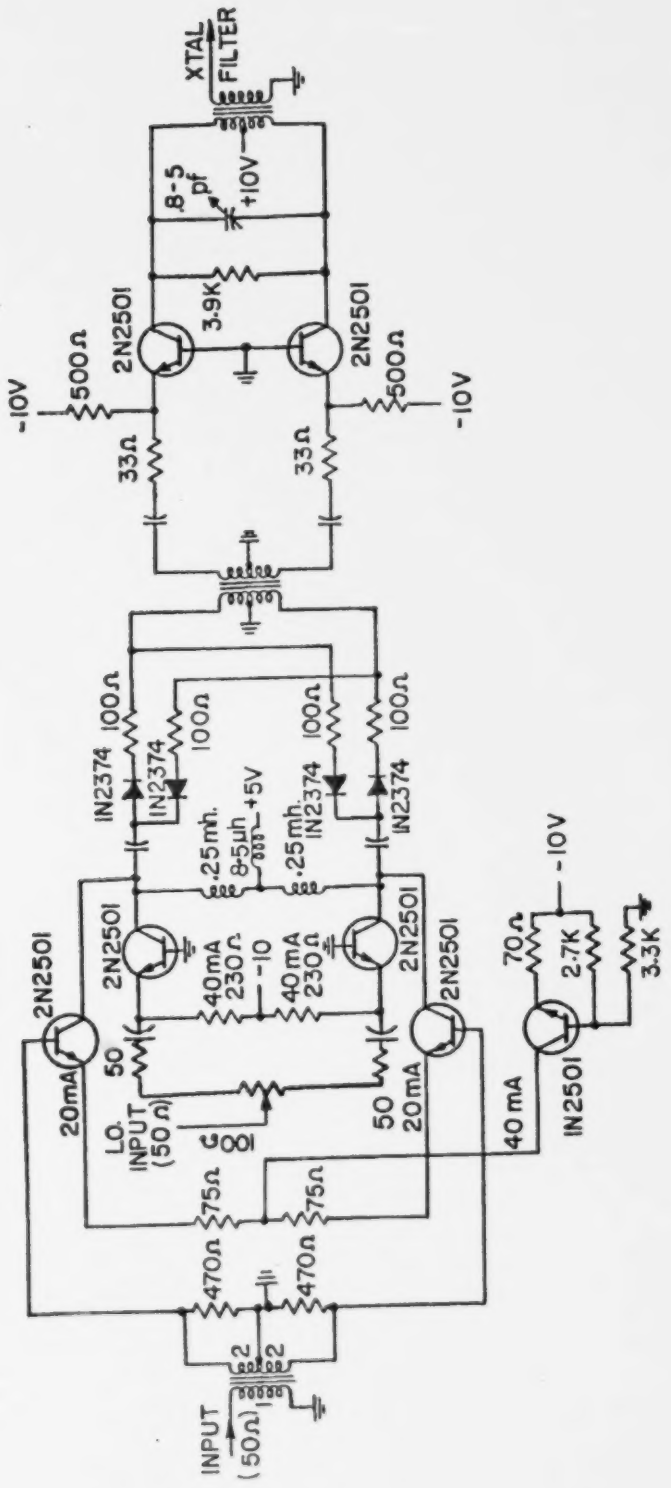

Fig. 13. Mixer assembly.

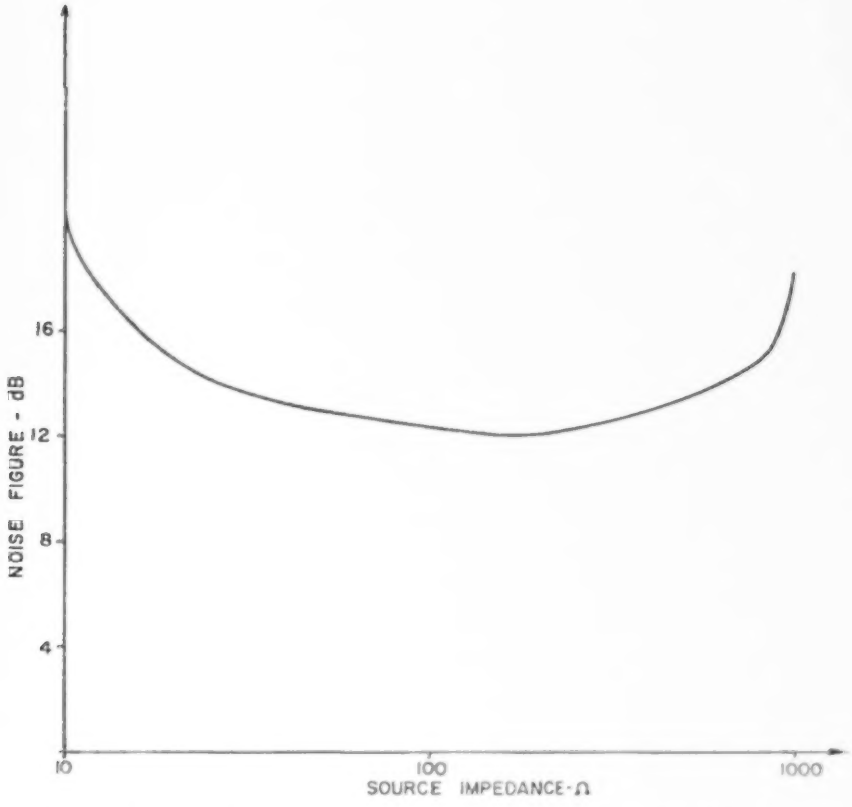

Fig. 14. Output buffer noise figure versus source impedance.

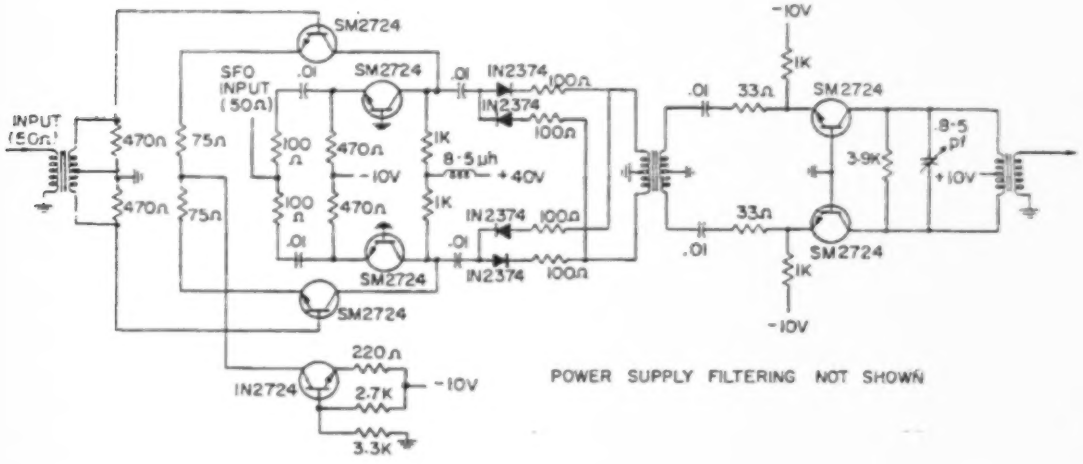

Fig. 15. Ring mixer and buffer.

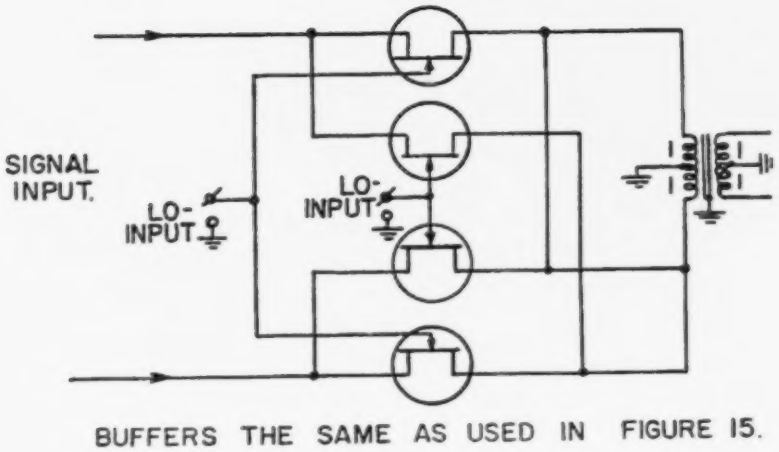

Fig. 16. Field effect transistor mixer.

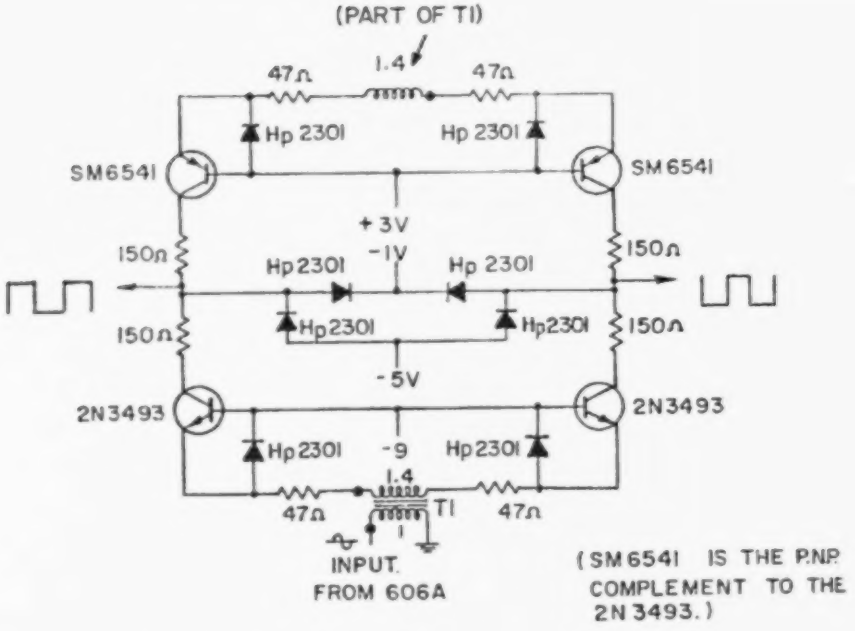

Fig. 17. Local oscillator square wave driver.

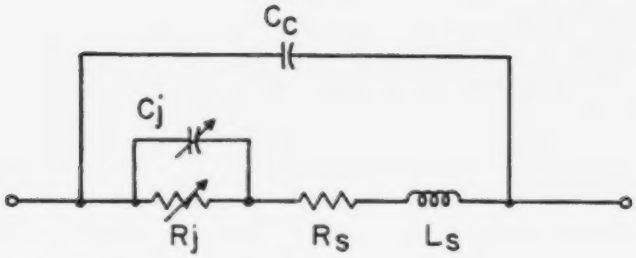

C_j - VOLTAGE VARIABLE JUNCTION CAPACITANCE.
R_S - SERIES RESISTANCE.
C_C - CASE CAPACITANCE.
L_S - SERIES INDUCTANCE.
R_j - VOLTAGE VARIABLE JUNCTION RESISTANCE.

Fig. 18. General equivalent for a reverse biased varactor diode.

C_j - VOLTAGE VARIABLE JUNCTION CAPACITANCE.
R_S - SERIES RESISTANCE.

Fig. 19. Low frequency equivalent for a reverse biased varactor diode.

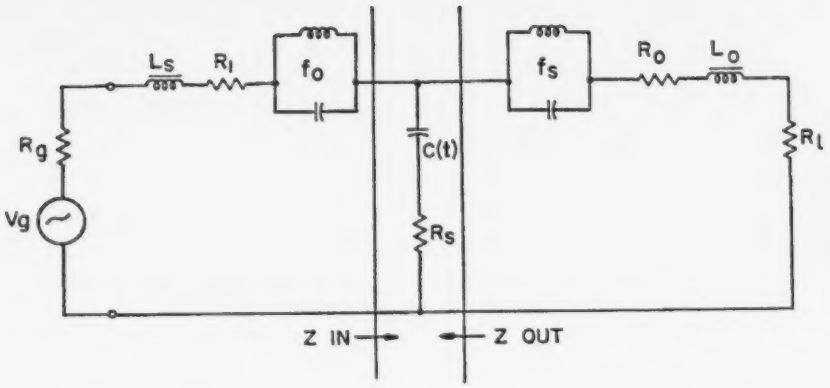

Fig. 20. Equivalent circuit for parametric up-converter.

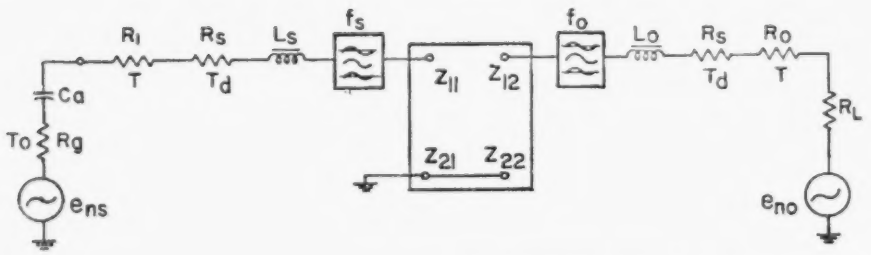

$e_{no}^2 = 4kB\,(T_d R_s + T \cdot R_o)$.
$e_{ns}^2 = 4kB\,(T_o R_g + T_d \cdot R_s + T R_l)$.
T_o = 290° K.
T_d = DIODE TEMPERATURE.
T = CIRCUIT TEMPERATURE.

Fig. 21. Equivalent for noise calculations.

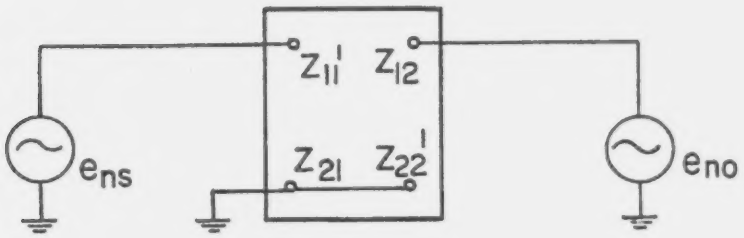

Fig. 22. Equivalent for noise calculation.

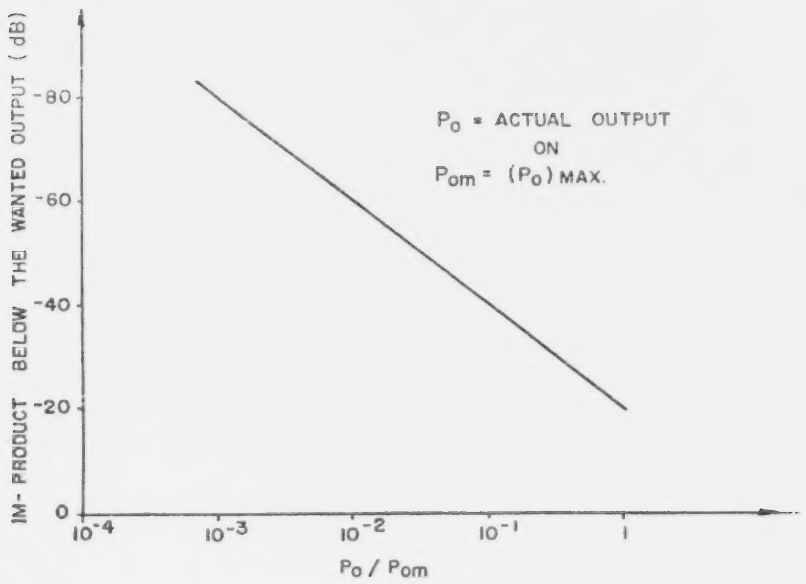

Fig. 23. Third order intermodulation in a parametric up-converter using abrupt junction diodes.

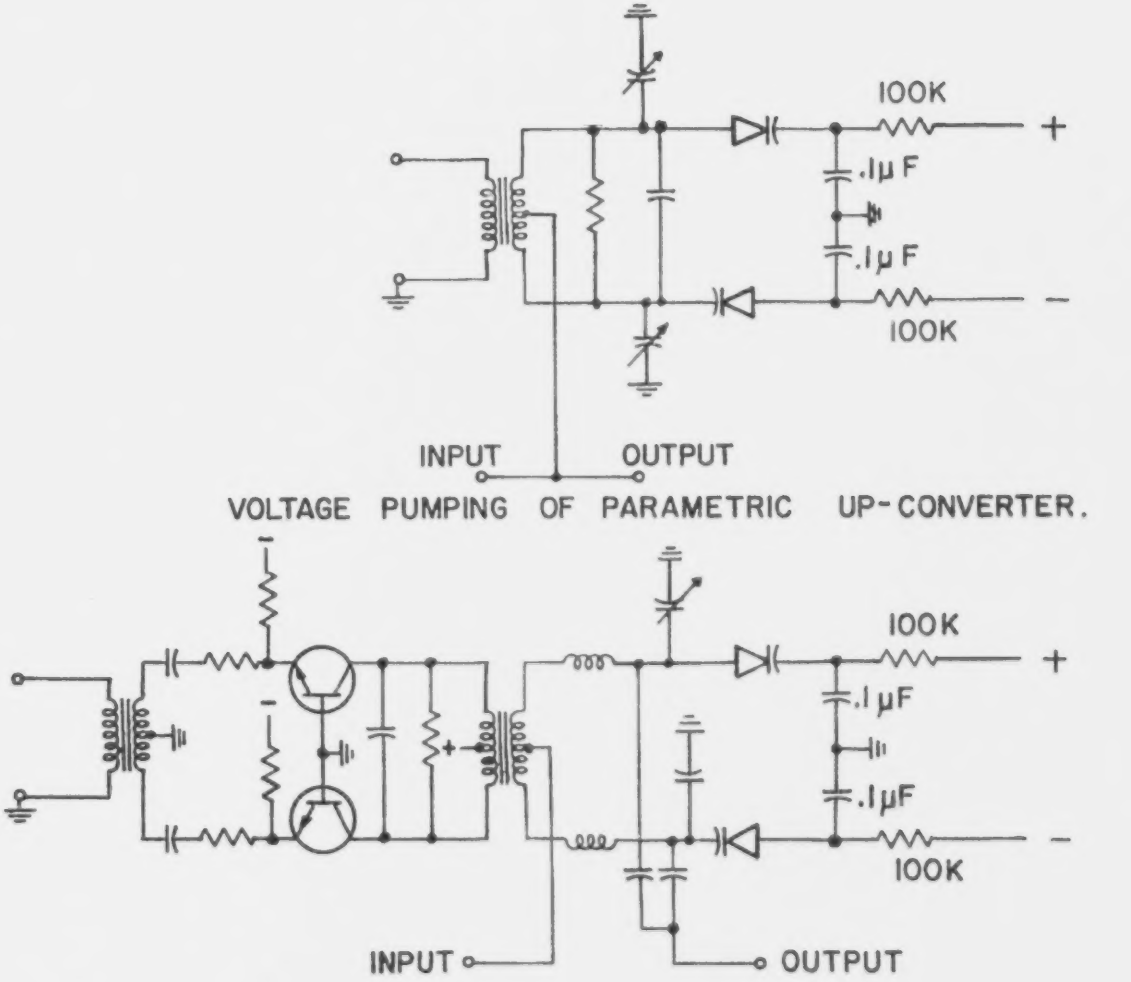

Fig. 24. Typical pumping schemes for parametric up-converter.

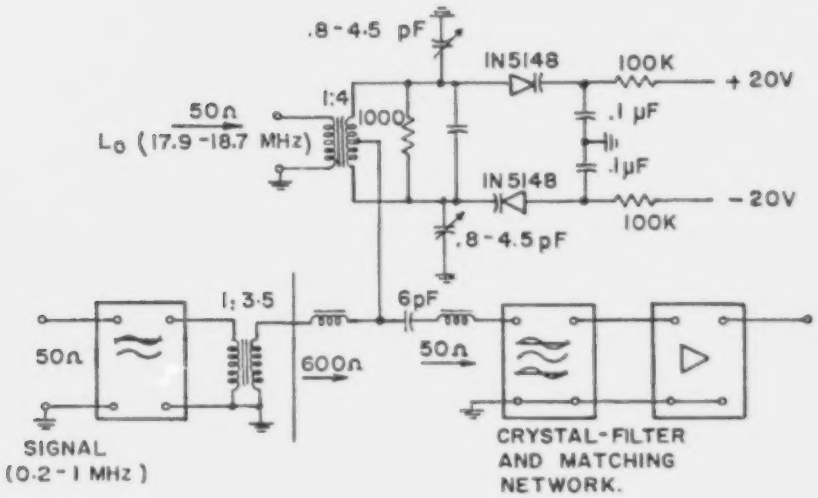

Fig. 25. Parametric up-converter.

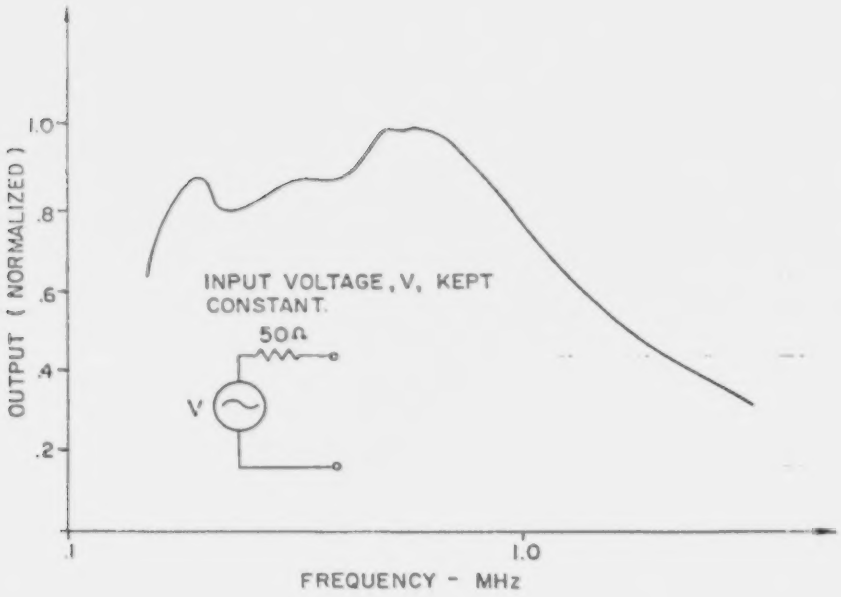

Fig. 26. Conversion of parametric up-converter shown in Fig. 25.

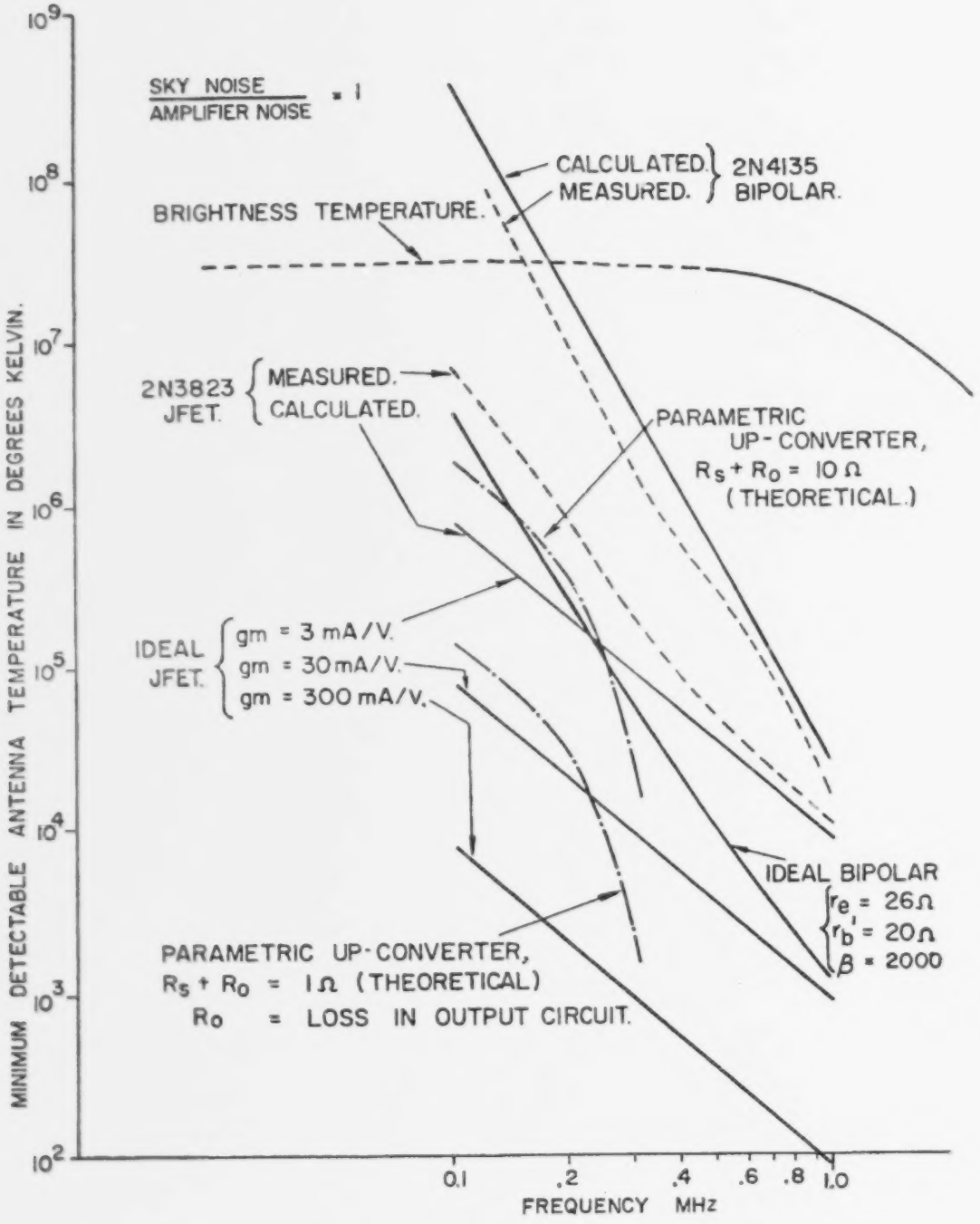

Fig. 27. Minimum detectable sky temperature for 240 foot dipole.

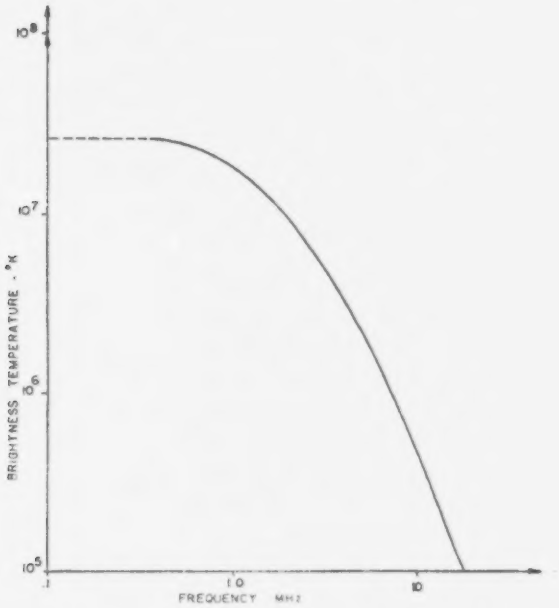

Fig. 28. Brightness temperature from cosmic noise versus frequency (from reference 23).

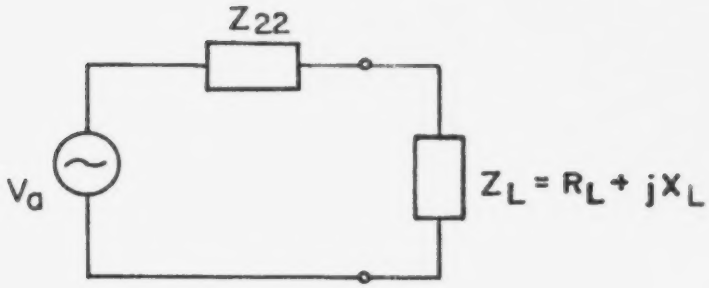

Fig. 29. Antenna equivalent.

Table 1. Intermodulation of common base amplifiers.

	F_0 MHz	F_1 MHz	F_2 MHz	Reference Level	Intermodulation: Single Ended	Compensated Single Ended	Push Pull	Compensated Push Pull
2nd order IM	3.5	6.0	9.5	1 μv	73 db	91 db	90 db	91 db
	3.5	9.5	13.0	1 μv	72 db	84 db	87.5 db	87.5 db
	.9	3.0	3.9	1 μv	73 db	89 db	90 db	91 db
	.9	4.0	4.9	1 μv	74 db	90 db	90 db	93 db
				(into 50 ohm)				
3rd order IM	3.5	8.0	12.5	1 μv	88 db	88 db	88 db	87 db
	3.5	6.0	15.5	1 μv	87 db	88 db	88 db	87 db
	.9	3.0	5.1	1 μv	88 db	89 db	86 db	87 db
	.9	4.0	7.1	1 μv	88 db	89 db	86 db	87 db
				(into 50 ohm)				

Table 2. Intermodulation of differential amplifier.

	F_0(MHz)	F_1(MHz)	F_2(MHz)	Reference	$R_1=R_2=56$ ohm	$R_1=R_2=75$ ohm	$R_1=R_2=100$ ohm
2nd order IM	3.5	6.0	9.5	1 μv	88 db	89 db	92 db
	3.5	9.5	13 0	1 μv	86 db	85 db	90.5 db
	.9	3.0	3.9	1 μv	87 db	93 db	93 db
	.9	4.0	4.9	1 μv	86.5 db	93 db	93 db
3rd order IM	3.5	8.0	12.5	1 μv	81 db	83 db	86 db
	3.5	6.0	15.5	1 μv	81 db	82 db	86 db
	.9	3.0	5 1	1 μv	81 db	83 db	86 db
	.9	4.0	7 1	1 μv	81 db	83 db	86 db

Table 3. Second order intermodulation comparison of switching elements.

Local Oscillator Frequency (MHz)			19.5		21		24	29	34	
Frequency F_1(MHz)			10	1.2	3.8	10	3	2	3	7
Frequency F_2(MHz)			10.5	1.7	5.8	12	8	8	18	8
	Drive Current mA(peak)	Series Resistance	Intermodulation above 1 μv (db)							
HP 2374	23	none	73	74	79	79	75	73	76	72
1N6009	23	none	70	70	74	78	70	73	76	75
2N3493 *	33	none	75	73	77	82	72	68	70	68

* - "0-pF" transistor diode connected (collector-base)
The local oscillator potentiometer was adjusted for interfering frequencies F_1 = 10 MHz and F_2 = 12 MHz and then locked.

Table 4. Second order intermodulation comparison of series resistance.

Local Oscillator Frequency (MHz)			19.5		21		24	29	34	
Frequency F_1(MHz)			10	1.2	3.8	10	3	2	3	7
Frequency F_2(MHz)			10.5	1.7	5.8	12	8	8	18	8
	Drive Current mA(peak)	Series Resistance	Intermodulation above 1 μv (db)							
HP 2374	23	none	73	74	79	79	75	73	76	72
HP 2374	23	10 ohm	75	78	73	85	78	74	72	70
HP 2374	25	100 ohm	75	75	75	77	76	77	81	85

Table 5. Second order intermodulation versus drive level.

Local Oscillator Frequency (MHz)			19.5		21		24	29	34	
Frequency F_1 (MHz)			10	1.2	3.8	10	3	2	3	7
Frequency F_2 (MHz)			10.5	1.7	5.8	12	8	8	18	8
	Drive Current mA (Peak)	Series Resistance	Intermodulation above 1 μV							
HP 2374	13.6	100 ohm	85 db	82 db	79 db	88.5db	78 db	80 db	85 db	88 db
HP 2374	25	100 ohm	75 db	75 db	75 db	77 db	76 db	77 db	81 db	85 db
HP 2374	42	100 ohm	81 db	85 db	83 db	89 db	77 db	77 db	75 db	74 db

* The local oscillator potentiometer was adjusted for interfering frequencies F_1 = 10 MHz and F_2 = 12 MHz and then locked.

Table 6. Additional second order intermodulation measurements.

Local Oscillator Frequency (MHz)			19.5		21		24	29	34	
Frequency F_1 (MHz)			10	1.2	3.8	10	3	2	3	7
Frequency F_2 (MHz)			10.5	1.7	5.8	12	8	8	18	8
	Drive Current mA (peak)	Series Resistance	Intermodulation above 1 μV							
HP 2374	6.5	none	72 db	80 db	79 db	79 db	70 db	71 db	74 db	71 db
HP 2374	3.5	10 ohm	74 db	67 db	81.5db	85 db	70 db	65 db	78 db	82 db
HP 2374	12	39 ohm	78 db	80 db	84 db	86 db	82 db	76 db	80 db	78 db
HP 2374	13.6	100 ohm	85 db	82 db	79 db	88.5db	78 db	80 db	86 db	88 db
2N3493	7	none	70 db	70 db	71 db	75 db	78 db	74 db	60 db	58 db

* The local oscillator potentiometer was adjusted for interfering frequencies F_1 = 10 MHz and F_2 = 12 MHz and then locked.

Table 7. Noise figure of mixer assembly.

Local Oscillator Frequency	MHz 34	MHz 25	MHz 20	Local Oscillator (peak through each diode)
HP 2374 and no resistors	db	db	db	MA
	12.5	13.0	14.0	6.3
HP 2374 and 39 ohm resistors	12.0	12.5	13.0	12
HP 2374 and 100 ohm resistors	12.5	12.0	13.0	13.6
IN6009 and no resistors	13.5	13.5	14.0	23
2N3494 and no resistors	14.5	14.0	14.0	33.6

Table 8. Second order intermodulation for different local oscillator impedances.

Local Oscillator Frequency (MHz)			19.5		21		24	29	34	
Frequency F_1(MHz)			10	1.2	3.8	10	3	2	3	7
Frequency F_2(MHz)			10.5	1.7	5.8	12	8	8	18	8
	Drive Current mA(peak)	Series Resistance	Intermodulation above 1 μv (in db)							
HP 2374 (without heat sinks) On LO Buffer	13.6	100 ohm	84	81	81	85	79	75	77	79
HP 2374 (with heat sink on) LO Buffer Transistors	13.6	100 ohm	85	82	79	88.5	78	80	86	88
HP 2374 (with heat sinks) On LO Buffer Transistors The signal choke was replaced with two 1K res. and the DC-current through the LO-transistors was 20 mA	13.6	100 ohm	85	84	83	86	82	75	76	78

The LO potentiometer was adjusted for interfering frequencies F_1 = 10 (MHz) and F_2 = 12 (MHz) and then locked

Table 9. Second order intermodulation in field effect transistor mixers.

F_0 MHz	F_1 MHz	F_2 MHz	IM Above 1 μV	
			1551	2N3823
.5	.2	.7	54 db	68 db
	10.2	10.7	66 db	65 db
	15.2	15.7	69 db	67 db
2.1	.5	2.6	70 db	63 db
	5.2	7.3	69 db	63 db
	14.2	16.3	73 db	66 db
5	.4	5.4	73 db	64 db
	5.2	10.2	71 db	64 db
	10.2	15.2	75 db	66 db
10.2	.5	10.7	68 db	67 db
	4.3	14.5	70 db	71 db
15	.5	15.5	66 db	70 db
	7	8	66 db	66 db

Table 10. Intermodulation in parametric up-converter.

2nd Order IM Above 1 μV			
F_0 MHz	F_1 MHz	F_2 MHz	IM
3	4.1	1.1	82 db
2	3.6	1.6	78 db
2	4.1	2.1	80 db

3rd Order IM Above 1 μV			
F_0 MHz	F_1 MHz	F_2 MHz	IM
3.0	2.4	1.8	79 db
3.0	2.6	2.2	73 db
3.0	2.8	2.6	73 db
3.0	3.2	3.4	75 db
3.0	3.3	3.6	78 db
3.0	3.4	3.8	80 db
3.0	3.5	4.0	82 db
3.0	3.6	4.2	83 db

Defence Research and Development Canada | Recherche et développement pour la défense Canada

Canada

Français | Contact Us | Help | Search | Canada Site

Home | Defence R&D Canada | Defence Site

Browse Indexes

Titles

Authors

Descriptors

Corporate Authors

Corporate Acronyms

Report Numbers

Search Database

Summary

Prior Top **Document:** 1 of 2 Bottom Next Click here to Order Click here to Download

TITLE:(U) NOISE AND INTERMODULATION IN THE IONOSPHERIC SOUNDER RECEIVER FOR THE ALOUETTE AND ISIS SATELLITES

PERSONAL AUTHOR: Endresen, T.

CORPORATE AUTHOR: Defence Research Telecommunications Establishment, Ottawa ONT (CAN) Electronics Lab

ABSTRACT: (U) The problems associated with sounding the topside of the ionosphere over a wide frequency range with limited transmitter power and a long extendible electric dipole antenna system are described. estimated interference levels from ground based HF TRANSMITTERS AND NOISE FIGURES FOR VARIOUS RECEIVER FRONT-ENDS ARE GIVEN. Intermodulation and noise characteristics for different transistor amplifiers, resistive mixers and parametric up-converters are also given.

DESCRIPTORS: (U) Scientific satellites;Topside sounders;Radio receivers

REPORT NUMBER: TN607;	**REPORT DATE:** 15 Feb 1969	**NUMBER OF PAGES :** 65
DRDKIM N°: 69-03830	**CANDIS N°:** 73528	**Format(s):**Hardcopy;Originator's fiche received by DSIS;Document Image stored on Optical Disk

Date modified: 2003-04-17

It is recommended you search "Authors" and "Corporate Authors" on their respective "Browse" pages.

Click here if you are having problems displaying text (ie. text is too big, or too small) or page appears to be jumbled.

Important Notices